

RESEARCH

Open Access



# Variations in the archaeal community and associated methanogenesis in peat profiles of three typical peatland types in China

Xuhui Chen<sup>1,2,7</sup>, Dan Xue<sup>1,2\*</sup>, Yue Wang<sup>1,7</sup>, Qing Qiu<sup>1,2,7</sup>, Lin Wu<sup>3</sup>, Meng Wang<sup>4</sup>, Jiawen Liu<sup>5</sup> and Huai Chen<sup>1,2,6\*</sup>

## Abstract

**Background** Peatlands contain about 500 Pg of carbon worldwide and play a dual role as both a carbon sink and an important methane (CH<sub>4</sub>) source, thereby potentially influencing climate change. However, systematic studies on peat properties, microorganisms, methanogenesis, and their interrelations in peatlands remain limited, especially in China. Therefore, the present study aims to investigate the physicochemical properties, archaeal community, and predominant methanogenesis pathways in three typical peatlands in China, namely Hani (H), Taishanmiao (T), and Ruokeba (R) peatlands, and quantitatively determine their CH<sub>4</sub> production potentials.

**Results** These peatlands exhibited high water content (WC) and total carbon content (TC), as well as low pH values. In addition, R exhibited a lower dissolved organic carbon concentration (DOC), as well as higher total iron content (TFe) and pH values compared to those observed in T. There were also clear differences in the archaeal community between the three peatlands, especially in the deep peat layers. The average relative abundance of the total methanogens ranged from 10 to 12%, of which *Methanosarcinales* and *Methanomicrobiales* were the most abundant in peat samples (8%). In contrast, *Methanobacteriales* were mainly distributed in the upper peat layer (0–40 cm). Besides methanogens, *Marine Benthic Group D/Deep-Sea Hydrothermal Vent Euryarchaeotic Group 1 (MBG-D/DHVEG-1)*, *Nitrosotales*, and several other orders of *Bathyarchaeota* also exhibited high relative abundances, especially in T. This finding might be due to the unique geological conditions, suggesting high archaeal diversity in peatlands. In addition, the highest and lowest CH<sub>4</sub> production potentials were 2.38 and 0.22 μg g<sup>-1</sup> d<sup>-1</sup> in H and R, respectively. The distributions of the dominant methanogens were consistent with the respective methanogenesis pathways in the three peatlands. The pH, DOC, and WC were strongly correlated with CH<sub>4</sub> production potentials. However, no relationship was found between CH<sub>4</sub> production potential and methanogens, suggesting that CH<sub>4</sub> production in peatlands may not be controlled by the relative abundance of methanogens.

**Conclusions** The results of the present study provide further insights into CH<sub>4</sub> production in peatlands in China, highlighting the importance of the archaeal community and peat physicochemical properties for studies on methanogenesis in distinct types of peatlands.

**Keywords** Peatland, Methane, Archaeal community, Peat properties, Methanogenesis

\*Correspondence:

Dan Xue

xuedan@cib.ac.cn

Huai Chen

chenhuai@cib.ac.cn

Full list of author information is available at the end of the article



© The Author(s) 2023. **Open Access** This article is licensed under a Creative Commons Attribution 4.0 International License, which permits use, sharing, adaptation, distribution and reproduction in any medium or format, as long as you give appropriate credit to the original author(s) and the source, provide a link to the Creative Commons licence, and indicate if changes were made. The images or other third party material in this article are included in the article's Creative Commons licence, unless indicated otherwise in a credit line to the material. If material is not included in the article's Creative Commons licence and your intended use is not permitted by statutory regulation or exceeds the permitted use, you will need to obtain permission directly from the copyright holder. To view a copy of this licence, visit <http://creativecommons.org/licenses/by/4.0/>. The Creative Commons Public Domain Dedication waiver (<http://creativecommons.org/publicdomain/zero/1.0/>) applies to the data made available in this article, unless otherwise stated in a credit line to the data.

## Introduction

Climate change has attracted considerable attention from researchers worldwide due to its great impacts on natural ecosystems and human society [1–3], with more and more climate-associated studies carried out [4–6]. Indeed, comprehensive studies on greenhouse gas emissions are of great significance to better understand climate change and accurately predict future trends of global warming [3, 7, 8].

Methane (CH<sub>4</sub>) is the second most abundant greenhouse gas after CO<sub>2</sub>, contributing to the radiative force increase in the lower atmosphere by about 20% [8, 9]. The global warming potential (GWP) of CH<sub>4</sub> is about 28 times higher than that of CO<sub>2</sub> over a 100-year time horizon [3, 10, 11]. In addition, the CH<sub>4</sub> concentration in the atmosphere has increased by at least 2.5 times since the first industrial revolution in 1750 and is predicted to reach 2000 ppb by 2030 [8, 12].

Peatland is an important carbon sink worldwide, stocking about 500 Pg of carbon, even though it covers 3% of the land surface [13, 14]. However, peatland can also be a potential source of CH<sub>4</sub>, with an estimated annual CH<sub>4</sub> flux of about 3.6 mg m<sup>-2</sup> [15], emitting approximately 126 Tg CH<sub>4</sub> per year, which contributes to at least 50 and 14–27% of CH<sub>4</sub> emitted from wetlands and global, respectively [16–18]. Therefore, investigating peatland-climate links is of great significance for predicting future climate change, as well as for the fate and evolution of peatlands.

Peatlands can be generally classified as minerotrophic fen, ombrotrophic bog, and other intermediate types depending on the climatic, hydrological, and topographical conditions [13, 19, 20]. Indeed, there are significant differences between minerotrophic fens and ombrotrophic bogs. For example, the pH of minerotrophic fens is higher than that of ombrotrophic bogs due to the mineral enrichment from groundwater [21, 22], while atmospheric precipitation dominates in ombrotrophic bogs, resulting in low pH values [15, 23]. Subsequently, the water recharge and pH conditions can further influence vegetation colonization, as grass-sedge and *Sphagnum* dominates in fens and bogs, respectively, reflecting their nutrient conditions [13, 19, 24].

According to Kolka et al. [15] about 90% of peatlands are located in boreal regions, making these regions research hotspots. However, peatlands in China receive considerably less attention from researchers, although they cover an area of more than 10<sup>5</sup> km<sup>2</sup> [19]. Peatlands in China are mainly distributed in the Eastern Tibetan Plateau, Yungui Plateau, Coastal Plain of Fujian-Guangdong, Yangtze Plain, and the Northeast Region [25], covering various peatland types [25–27]. However, systematic studies on CH<sub>4</sub> production processes in these

regions are limited. Moreover, it is necessary to determine the ecological attribute of peatlands to better understand their potential contributions to the carbon cycle and future climate change in China.

CH<sub>4</sub> production in peatlands is quite different from CH<sub>4</sub> emission, as most of the CH<sub>4</sub> produced in peatlands is consumed by microbes, then the remaining amount can eventually be emitted to the atmosphere [28–30]. Therefore, CH<sub>4</sub> production is the primary and direct factor of CH<sub>4</sub> emission in peatlands. In nature, CH<sub>4</sub> is produced by methanogens from seven orders of *Euryarchaeota*, namely *Methanobacteriales*, *Methanococcales*, *Methanopyrales*, *Methanosarcinales*, *Methanomicrobiales*, *Methanocellales*, and *Methanomassiliicoccales* [31–33]. However, new archaea that can also produce CH<sub>4</sub> have recently been identified, such as *Methanomethyliales* and *Methanofastidiosales*, as well as several species belonging to *Bathyarchaeota* [32, 33]. Although there are various methanogens in taxonomy, the metabolic pathways of CH<sub>4</sub> production can be generally classified as hydrogenotrophic, acetotrophic, methylotrophic, methoxydotrophic, and alkylotrophic methanogenesis, according to the substrates used for metabolisms [34–37]. Peatlands provide anoxic environments in which methanogens are highly adapted due to the permanent water-saturated conditions [13, 34]. Therefore, it is important to explore the ecological and biological controls associated with CH<sub>4</sub> production in peatlands.

Several factors affect CH<sub>4</sub> production in peatlands, including temperature [38–40], hydrological characteristics [41, 42], and electron acceptor availability [43–45]. However, these factors cannot comprehensively explain CH<sub>4</sub> production in peatlands [44, 46–48]. Therefore, further comprehensive studies are required to reveal the mechanisms controlling CH<sub>4</sub> production in peatlands. In addition, further studies on the investigation of the main factors controlling CH<sub>4</sub> production in peatlands at the microbial scale are required to determine the relationships between biological and ecological functions, as well as the corresponding processes in peatlands.

The present study aims to explore the potential impacts of methanogens, as well as other archaea, and basic physicochemical properties on CH<sub>4</sub> production in three typical peatlands in China. The differences in the archaeal community and CH<sub>4</sub> production processes were determined in this study to reveal the characteristics of the archaeal community associated with CH<sub>4</sub> production in the study areas. Here, we hypothesize that the archaeal communities are substantially distinct among three typical peatland types, and the differences of methanogenesis among them can be explained by the physicochemical properties and the archaeal communities.

## Materials and methods

### Study area

In this study, we selected three typical peatlands in China (Fig. 1a), namely Hani (H), Taishanmiao (T), and Ruokeba (R) peatlands. H is located in Tonghua City, Jilin Province, in the western part of Changbai Mountain (Fig. 1b and c). The selected peatland covers an area of about 18 km<sup>2</sup> at 926 m asl [49]. The basement is constituted by volcanic eruption-derived basalt during the Cenozoic Era, and the thickness of the peat layer can reach several meters [50, 51]. Sedge-*Sphagnum* is the dominant vegetation species in this study area [27, 50–52] H can be classified as a poor fen. T is located in Enshi Tujia and Miao Autonomous Prefecture, Hubei Province at 1826 m asl (Fig. 1d and e). This peatland is comparatively recent

and unevenly distributed, with thickness of peat hardly exceeding 1 m. *Sphagnum* is the absolute dominant plant [27]. Underground karst topography may have impact on this peatland [26, 27]. T can be classified as an ombrotrophic bog. R is located in Ngawa Tibetan and Qiang Autonomous Prefecture, Sichuan Province, in the southern part of the Zoige Basin at 3467 m asl (Fig. 1d and f). Precipitation events occur mainly in summer. This peatland receives few disturbances from human activities, with a comparatively long development period. The thickness of the peat layer can reach several meters [53]. The vegetation in R is dominated by sedge and grass. R is classified as a minerotrophic fen. More detailed information about the three peatlands can be found in Additional file 1: Table S1.

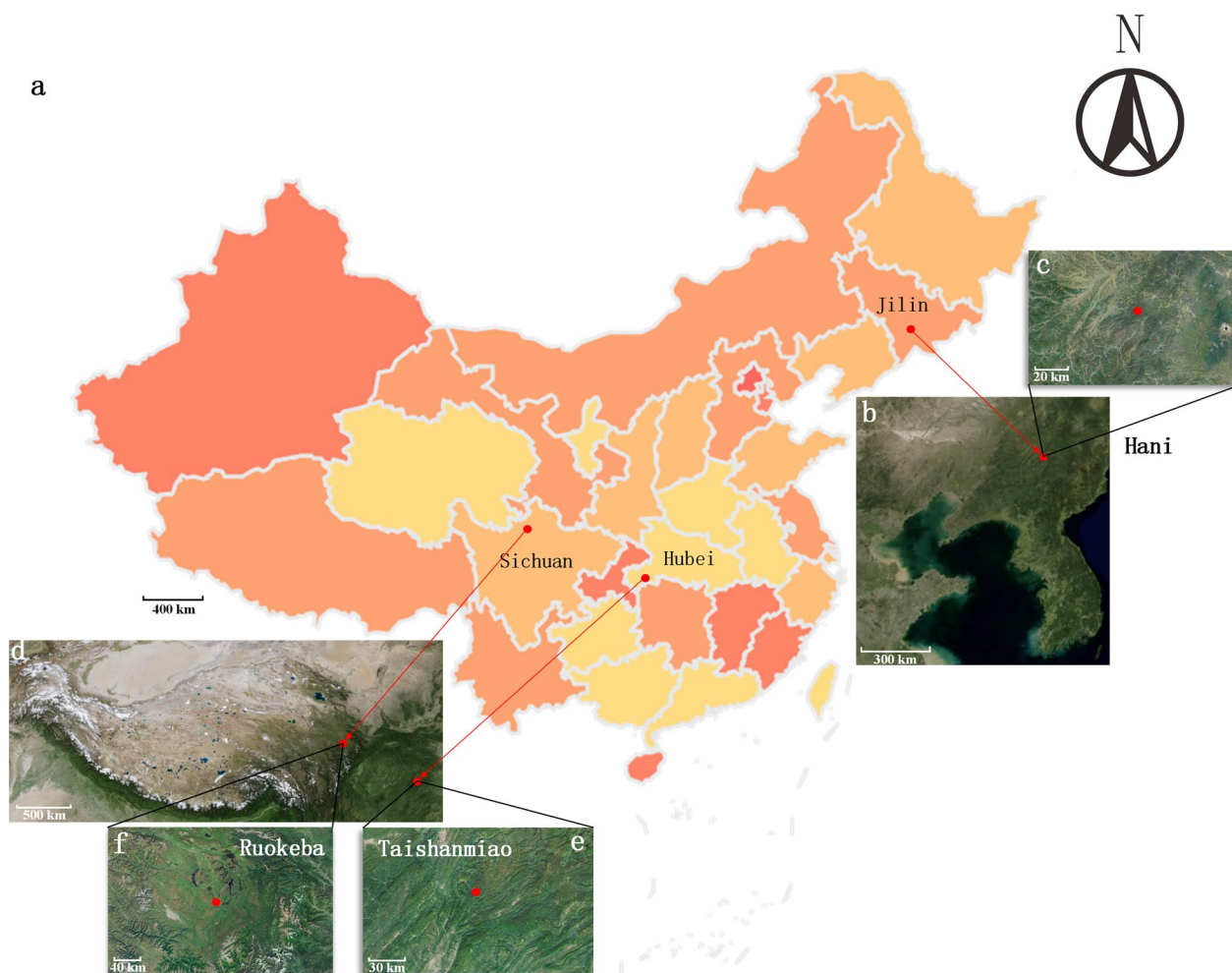


**Fig. 1** Geographic locations of the sampling sites in China. **a** Administrative map of China; **b** Satellite images of Bohai Bay and the Eastern Liaoning Peninsula; **c** Satellite image of Hani peatland; **d** Satellite image of Qinghai-Tibet Plateau; **e** Satellite image of Taishanmiao peatland; **f** Satellite image of Ruokeba peatland. Red points indicate the three sampling sites. The colors on the map indicate the provincial boundaries

### Collection and preparation of peat samples

Peat soil samples were collected from H and T during the growing season in 2020, and R in 2019. Indeed, 3 sampling sites on flat terrains, with similar vegetation composition and plant growing conditions, were randomly selected in this study. The distance between sampling sites was at least 20 m. Specifically, a 5 × 5 m quadrat was randomly placed at each site, from which five peat samples were collected following a diagonal sampling pattern, then mixed to obtain a composite sample from each sampling site. To obtain the complete characteristics of archaeal community along the peat profile across surface, transitional, and deep layers, we collected the 1 m-depth peat from three peatlands. Specifically, vegetation above the peat surface was first removed, then a stainless-steel soil drill was used to collect samples from five consecutive peat layers, namely 0–20, 20–40, 40–60, 60–80, and 80–100 cm. The peat samples were placed in plastic boxes and kept refrigerated, then immediately transferred to the laboratory.

In the laboratory, vegetation roots and debris were removed. A random part of each sample was placed in an ultra-low temperature freezer at –80 °C for microbiological analysis, while the remaining part of the peat sample was dried and sieved using a 2 mm plastic sieve. In addition, a part of each sieved soil sample was sieved through a 0.15 mm plastic sieve for physicochemical analyses.

### Determination of peat physicochemical properties

A portable pH meter (OxyScan 300, UMS GmbH & Co. KG., Germany) was used to determine the pH values of the peat samples. Whereas the gravimetric method was used to determine the peat water content (WC). Dissolved organic carbon (DOC) was determined by a total organic carbon (TOC) analyzer (vario TOC, Elementar Analysensysteme GmbH, Germany) after extraction with ultrapure water [54]. The total iron contents (TFe) in peat samples were determined using the ultraviolet spectrophotometry method [55]. Total carbon content (TC) and total nitrogen content (TN) were determined by the elementary analyzer (Vario Cube, Elementar Analysensysteme GmbH, Germany). The total phosphorus (TP) contents were determined using an elementary analyzer following extraction using the modified sulphuric acid-perchloric acid digestion method [56, 57].

### Incubation experiment

An incubation experiment was conducted in this study to quantify the CH<sub>4</sub> production potential of the three peatlands. All layers of peat in each peatland were first well-mixed to form a 1 m-depth integral sample. Peat samples (20 g) were placed into brown incubation flasks with 40 mL ultrapure water [58]. The headspace was purged

with nitrogen through a gas displacement device. In addition, a pre-incubation period of 7 days at 15 °C and under 150 rpm in the incubator shaker was considered in this study to ensure proper microbe activation and peat sample mixing [59]. The incubation experiment was conducted over 104 days and at 25 °C to obtain the potential of methane production. The gas in the headspace was collected weekly, then stored in vacuum tubes and analyzed using a gas chromatograph (Clarus 500, PerkinElmer Co., USA). The headspace in the flask was replaced by N<sub>2</sub> after gas sampling [58, 60].

The methanogenesis pathways were determined in the present study. 5 g of mixed peat samples were placed into 100 mL brown incubation flasks with 30 mL ultrapure water or solutions (M:V of 1:6) [58, 61]. Indeed, one control and three treatment groups were considered in the experiment. 30 mL ultrapure water was added to the control group (CK; 5 g peat + 30 mL water), while the three treatment groups consisted of methanol (Me; 5 g peat + 30 mL methanol), acetate (Ac; 5 g peat + 30 mL acetate), and sodium bicarbonate (CO<sub>2</sub>; 5 g peat + 30 mL sodium bicarbonate), with final solution concentrations of 0.02 mol L<sup>-1</sup> [62, 63]. Each group consisted of three parallel samples, which were incubated at 25 °C. Before incubation, the pH values of all samples were adjusted to the in-situ pH values [64]. For the CO<sub>2</sub> group, 10 mL of H<sub>2</sub> was injected following the replacement of headspace gas. The gas in the headspace was collected on 3, 7, 14, and 21 days of incubation and analyzed using a gas chromatograph.

### Metagenome sequencing

#### DNA extraction

The PowerSoil DNA Isolation Kit (MO BIO Laboratories Inc., the Netherlands) was used in this study to extract DNA from peat samples following the manufacturer's instructions. The extracted DNA was stored at –80 °C until further processing. The quantity and quality of the extracted DNA were determined by a NanoDrop 1000 (Thermo Fisher Scientific Co., USA) and 1.2% agarose gel electrophoresis, respectively.

#### Paired-end sequencing with illumina MiSeq

The TruSeq Nano DNA LT Library Prep Kit was used to prepare 16S rRNA gene sequencing libraries, following the Illumina official protocol (Illumina Co., USA). The 16S rRNA gene primer pair, 524F(5'-TGYCAGCCGCCG CGGTAA-3')/958R(5'-YCCGGCGTTGAVTCCAAT T-3'), was used to amplify the V4V5 regions. The paired-end libraries were then selected and purified through 2% agarose gel electrophoresis. Before sequencing, the quality of the libraries was tested using a High Sensitivity DNA Kit (Agilent Technologies Co., USA). The libraries

had only one single peak without adaptors. Next, a Promega QuantiFluor (Promega Co., USA) with Quant-iT PicoGreen dsDNA Assay Kit (Molecular Probes Co., USA) was used to quantify the selected libraries with concentrations  $\geq 2$  nmol L<sup>-1</sup>. All samples were first pooled in equimolar concentrations and denatured into single strands by NaOH solution, then sequenced on the Illumina MiSeq platform using MiSeq Reagent Kit V3 (600 cycles, Illumina Co., USA).

### Processing of sequencing data

The sequence data were processed using QIIME 2 2019.4 [65], with slight modifications to the official tutorials (<https://docs.qiime2.org/2019.4/tutorials/>). Raw sequence data were first demultiplexed and filtered using the demux plugin then the primers were cut using the cutadapt plugin [66]. All amplicon sequence variants (ASVs) were aligned with mafft via the q2-alignment plugin [67]. The q2-diversity plugin was used to estimate  $\alpha$ -diversity and  $\beta$ -diversity metrics of 900 sequences per sample with Bray–Curtis dissimilarity following sampling without replacement [68, 69]. Taxonomy was assigned to ASVs using the q2-feature-classifier plugin with 99% similarity in operational taxonomy units (OTUs) of sequence against the Greengenes 13\_8 database [70, 71].

### Data processing and analysis

The produced CH<sub>4</sub> amounts were estimated in this study using the following formula [58]:

$$P = c \cdot \frac{V}{W} \cdot \frac{MW}{MV} \cdot \frac{T_0}{T} \quad (1)$$

where P ( $\mu\text{g g}^{-1}$ ) denotes the CH<sub>4</sub> concentration in the headspace; c (ppmv) denotes the CH<sub>4</sub> concentration determined by gas chromatograph; V (L) denotes the volume of headspace; W (g) denotes the dry weight of the peat sample; MW (16 g mol<sup>-1</sup>) denotes the relative molecular mass of CH<sub>4</sub>; MV (22.4 L mol<sup>-1</sup>) denotes the molar volume of gas under standard conditions; T<sub>0</sub> (273.15 K) is the Kelvin temperature under standard conditions; T (K) is the incubation temperature.

The weekly CH<sub>4</sub> production rates were further summed to draw the accumulation–incubation time curve of CH<sub>4</sub>. The *grofit* R package was used to estimate the CH<sub>4</sub> production potential, representing the highest CH<sub>4</sub> rate [72]. For the methanogenesis pathway experiment, the accumulation–incubation time of CH<sub>4</sub> was fitted using linear regression, showing an average determination coefficient ( $R^2$ ) of 0.94. The average CH<sub>4</sub> production rate of each control group was used to normalize the values of corresponding samples in treatment groups to obtain relative methanogenesis values. This was only a qualitative

method to determine the dominant methanogenesis pathways in the three considered peatlands.

The  $\beta$ -diversity of archaea was determined using a non-metric multidimensional scaling (NMDS) conducted by the Bray–Curtis dissimilarity matrix based on the OTU of the archaeal community. Differences in archaea abundance between different areas were shown in this study using a heatmap, following data normalization using the Z-score method. In addition, clustering trees were performed in this study using the unweighted pair-group method with arithmetic means (UPGMA) based on the Bray–Curtis dissimilarity matrix of species and areas to reveal the similarity in the peat samples and the distributions of the archaeal community. Pearson correlation analysis was performed in this study using the *corrplot* package [73] in R [74].

Maps and satellite images were captured from DataV. GeoAtlas (Alibaba Cloud Computing Co., China). Statistical analyses, tables, and figures were all performed in Excel 2019 (Microsoft Co., USA), R v3.6.3 [74], and Visio 2019 (Microsoft Co., USA).

## Results

### Physicochemical properties of the three peatlands

The WC in H, T, and R was generally high, ranging from 300 to 700% in most peat soil samples (Table 1). TC showed an increasing trend with soil depth in both H and R, ranging from 20 to 40%. In contrast, a decreasing trend in the TC values was observed in T, varying from 30 to 9.66% (Table 1). The change in the TN content was similar to that of TC in the three peatlands, ranging from 0.61 to 2.20% (Table 1). The TP contents showed a decreasing trend with soil depth, ranging from 0.40 to 1.26%. However, this variation was not observed in H (Table 1). The carbon/nitrogen (C/N) values of R showed a significant increase with soil depth ( $p < 0.05$ ), varying from 15 to 18.61. In contrast, no significant differences in the C/N values were observed between the soil layers of the remaining peatlands, showing values of about 17 across the soil profiles (Table 1). In T, the DOC concentrations in the deep soil layers (40–100 cm) were significantly lower than those in the surface layers (0–20 cm,  $p < 0.05$ ), ranging from 1.13 to 3.04 mg g<sup>-1</sup>, while no significant differences in the DOC concentrations were observed between the soil layers in H and R (Table 1). Soils in R exhibited higher pH (mean 5.92) and TFe (mean 2.62 mg Fe g<sup>-1</sup>) than those observed in the other two peatlands, regardless of depth ( $p < 0.05$ , Table 1). In addition, the obtained results showed significantly higher TFe contents in the upper soil layer than those in the deeper soil layers in H and T ( $p < 0.05$ ). Whereas in T, significantly lower TFe contents in the upper soil layers than

**Table 1** Peat physicochemical properties in different peat layers in the three peatlands

Location	Depth (cm)	WC (%)	TC (%)	TN (%)	TP (mg g <sup>-1</sup> )	C/N	DOC (mg g <sup>-1</sup> )	pH	TFe (mg Fe g <sup>-1</sup> )
H	0–20	643.32 ± 12.87 <sup>ab</sup>	28.70 ± 0.77 <sup>c</sup>	1.67 ± 0.04 <sup>b</sup>	0.61 ± 0.07 <sup>a</sup>	17.18 ± 0.80 <sup>a</sup>	1.84 ± 0.32 <sup>a</sup>	5.71 ± 0.38 <sup>a</sup>	2.66 ± 0.74 <sup>a</sup>
H	20–40	539.65 ± 35.38 <sup>b</sup>	30.67 ± 0.1 <sup>bc</sup>	1.89 ± 0.10 <sup>ab</sup>	0.67 ± 0.06 <sup>a</sup>	16.33 ± 0.85 <sup>a</sup>	1.33 ± 0.27 <sup>a</sup>	4.97 ± 0.10 <sup>b</sup>	1.34*
H	40–60	644.64 ± 35.38 <sup>ab</sup>	34.00 ± 0.93 <sup>ab</sup>	2.10 ± 0.08 <sup>a</sup>	0.60 ± 0.07 <sup>a</sup>	16.20 ± 0.26 <sup>a</sup>	1.69 ± 0.15 <sup>a</sup>	5.12 ± 0.06 <sup>b</sup>	1.32 ± 0.13 <sup>b</sup>
H	60–80	631.58 ± 58.60 <sup>ab</sup>	34.22 ± 1.60 <sup>ab</sup>	2.00 ± 0.12 <sup>ab</sup>	0.56 ± 0.03 <sup>a</sup>	17.17 ± 0.54 <sup>a</sup>	1.59 ± 0.07 <sup>a</sup>	5.10 ± 0.08 <sup>b</sup>	1.35 ± 0.18 <sup>b</sup>
H	80–100	705.02 ± 41.32 <sup>a</sup>	36.54 ± 0.59 <sup>a</sup>	2.08 ± 0.09 <sup>a</sup>	0.55 ± 0.08 <sup>a</sup>	17.59 ± 0.80 <sup>a</sup>	1.88 ± 0.42 <sup>a</sup>	4.91 ± 0.09 <sup>b</sup>	1.50 ± 0.15 <sup>b</sup>
H	Mean	632.87 ± 66.30 <sup>A</sup>	32.83 ± 3.19 <sup>A</sup>	1.95 ± 0.21 <sup>A</sup>	0.60 ± 0.07 <sup>B</sup>	16.89 ± 1.15 <sup>A</sup>	1.67 ± 0.31 <sup>A</sup>	5.16 ± 0.33 <sup>B</sup>	1.60 ± 0.56 <sup>B</sup>
T	0–20	937.34 ± 191.97 <sup>a</sup>	30.90 ± 4.21 <sup>a</sup>	1.65 ± 0.20 <sup>a</sup>	0.91 ± 0.05 <sup>a</sup>	18.69 ± 0.26 <sup>a</sup>	3.04 ± 0.49 <sup>a</sup>	5.09 ± 0.23 <sup>a</sup>	2.10 ± 0.75 <sup>a</sup>
T	20–40	713.11 ± 361.53 <sup>ab</sup>	29.35 ± 6.23 <sup>a</sup>	1.64 ± 0.29 <sup>a</sup>	1.00 ± 0.05 <sup>a</sup>	17.69 ± 0.87 <sup>a</sup>	2.34 ± 1.18 <sup>ab</sup>	4.77 ± 0.31 <sup>a</sup>	0.73 ± 0.02 <sup>ab</sup>
T	40–60	345.84 ± 168.14 <sup>bc</sup>	22.50 ± 4.02 <sup>a</sup>	1.34 ± 0.28 <sup>a</sup>	0.96 ± 0.04 <sup>a</sup>	16.96 ± 0.55 <sup>a</sup>	1.25 ± 0.47 <sup>b</sup>	5.01 ± 0.14 <sup>a</sup>	0.57 ± 0.13 <sup>b</sup>
T	60–80	205.78 ± 102.93 <sup>bc</sup>	17.28 ± 6.63 <sup>a</sup>	0.96 ± 0.33 <sup>a</sup>	0.61 ± 0.14 <sup>ab</sup>	17.31 ± 0.99 <sup>a</sup>	1.13 ± 0.31 <sup>b</sup>	5.04 ± 0.22 <sup>a</sup>	0.39 ± 0.21 <sup>b</sup>
T	80–100	121.76 ± 124.82 <sup>c</sup>	9.66 ± 6.50 <sup>a</sup>	0.61 ± 0.33 <sup>a</sup>	0.40 ± 0.10 <sup>b</sup>	13.61 ± 2.36 <sup>a</sup>	1.28 ± 0.12 <sup>b</sup>	5.09 ± 0.34 <sup>a</sup>	0.52 ± 0.17 <sup>b</sup>
T	Mean	464.80 ± 368.10 <sup>B</sup>	21.94 ± 11.58 <sup>B</sup>	1.24 ± 0.60 <sup>B</sup>	0.78 ± 0.27 <sup>A</sup>	16.85 ± 2.54 <sup>A</sup>	1.81 ± 0.94 <sup>A</sup>	5.00 ± 0.25 <sup>B</sup>	0.87 ± 0.74 <sup>C</sup>
R	0–20	337.12 ± 16.05 <sup>a</sup>	28.33 ± 2.37 <sup>b</sup>	1.88 ± 0.11 <sup>ab</sup>	1.26 ± 0.05 <sup>a</sup>	14.99 ± 0.40 <sup>b</sup>	0.89 ± 0.07 <sup>a</sup>	5.83 ± 0.35 <sup>ab</sup>	3.14 ± 0.91 <sup>ab</sup>
R	20–40	341.34 ± 129.62 <sup>a</sup>	21.13 ± 2.20 <sup>b</sup>	1.42 ± 0.10 <sup>c</sup>	0.94 ± 0.19 <sup>b</sup>	14.80 ± 0.52 <sup>b</sup>	0.96 ± 0.27 <sup>a</sup>	5.57 ± 0.13 <sup>b</sup>	3.31 ± 0.96 <sup>a</sup>
R	40–60	304.94 ± 88.69 <sup>a</sup>	27.65 ± 0.63 <sup>b</sup>	1.64 ± 0.04 <sup>bc</sup>	0.71 ± 0.03 <sup>bc</sup>	16.93 ± 0.74 <sup>ab</sup>	1.01 ± 0.30 <sup>a</sup>	6.04 ± 0.05 <sup>ab</sup>	1.84 ± 0.06 <sup>b</sup>
R	60–80	379.24 ± 37.52 <sup>a</sup>	36.19 ± 0.94 <sup>a</sup>	1.96 ± 0.07 <sup>ab</sup>	0.60 ± 0.05 <sup>c</sup>	18.50 ± 0.64 <sup>a</sup>	1.27 ± 0.04 <sup>a</sup>	6.09 ± 0.17 <sup>a</sup>	2.29 ± 0.21 <sup>ab</sup>
R	80–100	467.17 ± 33.50 <sup>a</sup>	40.91 ± 0.83 <sup>a</sup>	2.20 ± 0.03 <sup>a</sup>	0.62 ± 0.04 <sup>c</sup>	18.61 ± 0.16 <sup>a</sup>	1.23 ± 0.04 <sup>a</sup>	6.06 ± 0.11 <sup>ab</sup>	2.52 ± 0.30 <sup>ab</sup>
R	Mean	366.00 ± 85.11 <sup>B</sup>	30.84 ± 7.55 <sup>A</sup>	1.82 ± 0.30 <sup>A</sup>	0.82 ± 0.27 <sup>A</sup>	16.76 ± 1.87 <sup>A</sup>	1.07 ± 0.22 <sup>B</sup>	5.92 ± 0.26 <sup>A</sup>	2.62 ± 0.76 <sup>A</sup>

Data were presented as mean ± 1 SD ( $n=3$ ). Different lowercase letters indicate significant differences in each parameter between peat layers in each peatland at the  $p < 0.05$  level, while the uppercase letters indicate significant differences in the average value of each parameter between the three peatlands at the  $p < 0.05$  level, regardless of depth, determined using the Tukey's HSD test, with  $p < 0.05$ . WC, TC, TN, TP, DOC, and TFe denote peat water content, total carbon content, total nitrogen content, total phosphorus content, dissolved organic carbon, and total Fe content, respectively. The C/N values were calculated using the mass ratio (TC/TN). H, T, and R denote Hani, Taishanmiao, and Ruokeba peatlands, respectively

\*This value was not considered in the ANOVA test due to sample replicate loss. Only a single value is presented

those in the deeper soil layers were observed ( $p < 0.05$ , Table 1).

### Archaeal community characteristics and compositions in the three peatlands

To better investigate the  $\beta$ -diversity of the archaeal community in the three peatlands, we established a nonmetric multidimensional scaling (NMDS) ordination (Fig. 2). This method intuitively exhibited a comparable archaeal community structure in the three peatlands in which the archaeal community became more distant with soil depth, showing a changing trend with peat depth. The projections of the archaeal community in T and R were set on the two opposite sides, while that in H was in the middle (Fig. 2).

To quantitatively assess the archaeal community composition, the top 20 orders of archaea were selected in this study based on their relative abundances (Fig. 3). In general, the dominant archaea were observed mainly in the upper layer of peat soil. There were seven orders of methanogens, with a total relative abundance range of 10–12% in each peatland. Indeed, five orders of these methanogens were included in the top seven orders in the archaeal community. Unlike *Methanobacteriales* that showed a high relative abundance in the 0–40 cm peat layer, *Methanosarcinales* and *Methanomicrobiales* were

abundant in all peat samples, while *Methanomassiliicoccales* exhibited a stable distribution across the peat profiles of the three peatlands, with relatively higher relative abundance in the 40–100 cm peat layer of R. A similar distribution was observed for *Methanomethyliales*. The relative abundances of *Methanocellales* and *Methanofastidiosales* were low in all peat samples (<1%). Besides methanogens, other archaeal communities might exhibit high relative abundances, especially in T, where the relative abundances of the *Marine Benthic Group D/deep-Sea Hydrothermal Vent Euryarchaeotic Group 1 (MBG-D/DHVEG-1)* and *Nitrosotaleales* reached an average value of 3.3%.

The differences in archaeal distribution between the three peatlands are shown in Fig. 4. Clustering results showed similar compositions of the dominant archaeal communities in the deep peat layer (60–100 cm) of H and R. For example, *Candidatus Bathyarchaeota Archaeon RBG\_16\_48\_13*, *Candidatus Methanomethylicus*, *Methanofollis*, *Methanolinea*, and *Methanomassiliicoccus* were more abundant in the deep peat layer of H. On the other hand, similar archaeal community compositions were observed in the upper peat layer (0–40 cm), where *Methanosarcina*, *Methanocella*, *Methanosaeta*, and others were the most abundant species. Furthermore, similar distribution patterns of the archaeal compositions

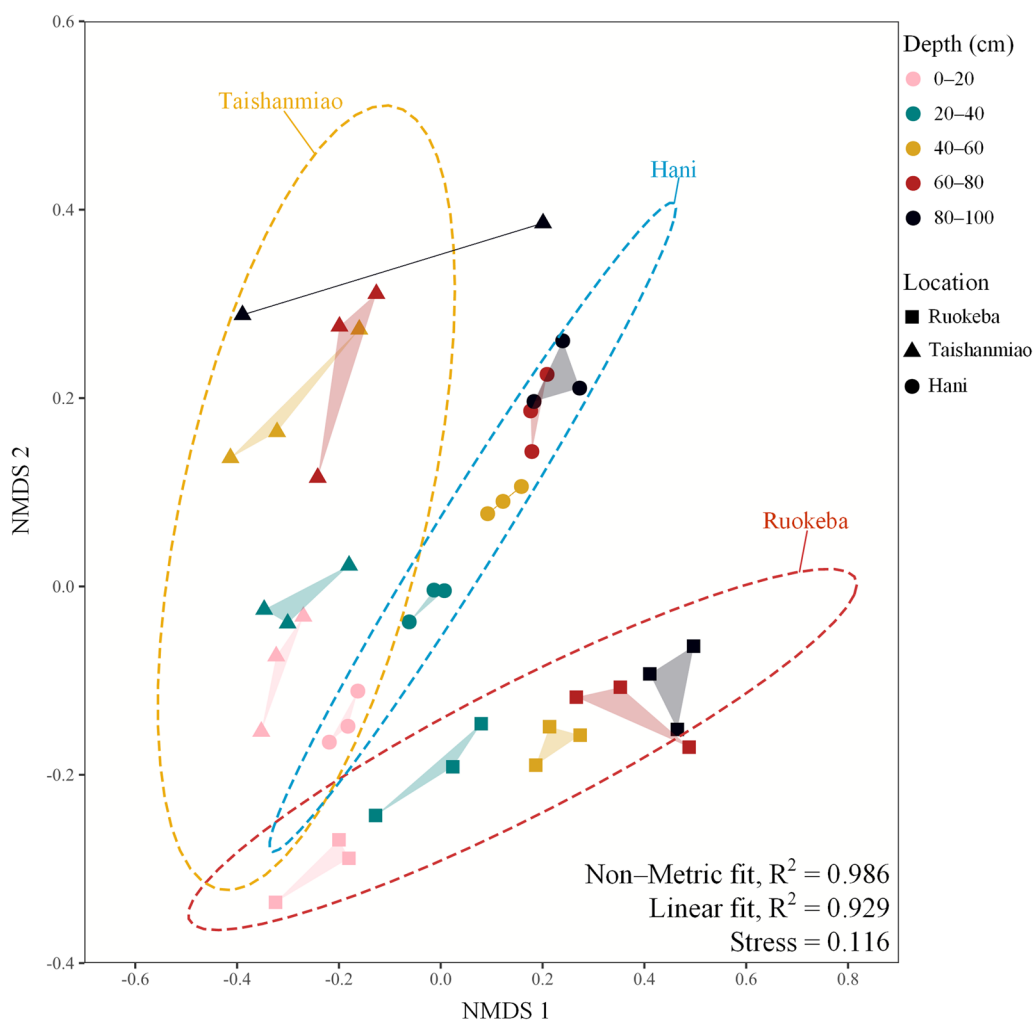


**Fig. 2**  $\beta$ -diversity of the archaeal community in the peat profiles in the three peatlands. It was determined by nonmetric multidimensional scaling (NMDS). Different color points represent different peat depths. Peat samples from Hani, Taishanmiao, and Ruokeba are indicated by circles, triangles, and squares, respectively. The  $R^2$  values were calculated based on the regression between ordination distance and observed original distance using the Shepard plot. Dashed ellipses indicate confidence intervals of samples from each peatland determined using the  $t$ -test ( $\alpha=0.05$ )

between the 40–100 cm and 20–60 cm peat layers in T and R, respectively, were observed.

#### Methane production potentials, dominant pathways, and influencing factors

The  $\text{CH}_4$  production potentials showed significant variations between the three peatlands. H exhibited a greater  $\text{CH}_4$  production potential than R and T ( $p < 0.05$ ), showing  $\text{CH}_4$  production potential values of 2.38, 0.22, and  $1.37 \mu\text{g}^{-1} \text{g}^{-1} \text{d}^{-1}$ , respectively (Fig. 5).

According to the relative methanogenesis, determined by the addition of substrates, hydrogenotrophic methanogenesis was the dominant pathway in H, showing a higher  $\text{CH}_4$  production rate than the control group by over 3.7 times ( $p < 0.001$ , Fig. 6a), while no significant

differences in the  $\text{CH}_4$  production rates between the remaining and control groups. A similar result was observed in T, showing greater methanogenesis in the  $\text{CO}_2$  group by about 2.5 times than that in the control group ( $p < 0.01$ , Fig. 6b). Unlike  $\text{H}_2/\text{CO}_2$  addition, methanol and acetate additions promoted  $\text{CH}_4$  production in R, of which methanogenesis with methanol was significantly more active ( $p < 0.001$ , Fig. 6c).

Several correlated indices with  $\text{CH}_4$  production potential were filtered in this study. Indeed, WC, pH, and DOC were the main factors associated with  $\text{CH}_4$  production potential (Table 2). The analysis of covariance showed a strong interaction between peat pH and the study areas ( $p = 0.005$ , Additional file 1: Tables S2 and S3). In terms of methanogens, a significant negative correlation was

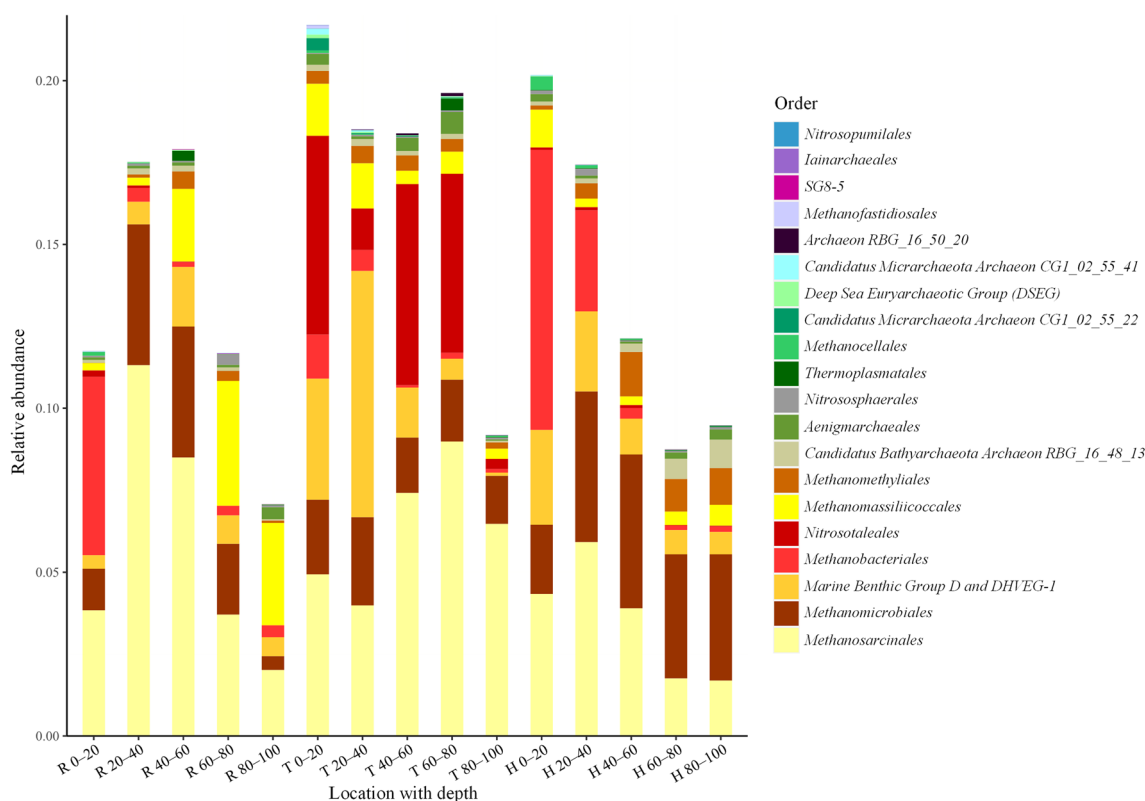


**Fig. 3** Relative abundances of the top 20 orders of archaea in the three peatlands. Different colors indicate different orders of archaea. The specific locations and peat layers (cm) are reported on the x-axis. R, T, and H denote Ruoqueba, Taishanmiao, and Hani, respectively

found between *Methanomassiliococcales* and  $\text{CH}_4$  production potential ( $R = -0.716$ ,  $p < 0.05$ , Table 2 and Additional file 1: Table S2).

#### Correlation analysis between peat physicochemical properties, archaeal community diversity indices, and archaeal abundances

To better demonstrate the interaction between the peat physicochemical properties and archaeal community, four representative indices characterizing  $\alpha$ -diversity of the archaeal community were extracted (Fig. 7). Chao1 and observed species represent the richness of archaea. According to the obtained results, Chao1 was significantly and negatively correlated with pH and TP ( $p < 0.05$ ), while the observed species showed a significant negative correlation with TP ( $p < 0.05$ ). The Simpson diversity index of archaea exhibited strong positive correlations with TC and TN ( $p < 0.01$ ), as well as with WC ( $p < 0.05$ ). Whereas Pielou's evenness index of the archaeal community was positively correlated with TN and WC ( $p < 0.05$ ). Seven archaea orders were incorporated in the analysis as the sum of their relative abundances accounted for 94% of the top 20 archaea orders (Figs. 3 and 7). Among them, *Methanomicrobiales* and

*Methanosarcinales* did not show any correlations with peat physicochemical parameters. *MBG-D/DHVEG-1* was negatively correlated with pH ( $p < 0.05$ ) and positively correlated with WC ( $p < 0.05$ ) and DOC ( $p < 0.01$ ). *Methanobacteriales* showed a strong positive correlation with TFe ( $p < 0.01$ ), while *Nitrosotaleales* and *Methanomethyliales* were negatively correlated with pH and TFe ( $p < 0.05$ ). *Methanomassiliococcales* exhibited significant positive correlations with TC ( $p < 0.05$ ), C/N ( $p < 0.01$ ), and pH ( $p < 0.001$ ).

A redundancy analysis (RDA) was performed in this study to further investigate the relationships between the physicochemical properties of peat samples, dominant archaea, and peatlands. The first two axes explained 20.28% (adjusted) of the total variance, of which the first (RDA1) and second (RDA2) axes explained 12.70 ( $p = 0.001$ ) and 7.58% ( $p = 0.009$ ) of the total variance, respectively (Additional file 1: Fig. S1). The projections of the study areas with depths characterized by physicochemical properties and dominant archaea showed that H was contained in R. However, the 60–100 cm layer in R was comparatively separate, while H and R were both distinguished from T (Additional file 1: Fig. S1). Furthermore, several archaea were region-specific. For example,

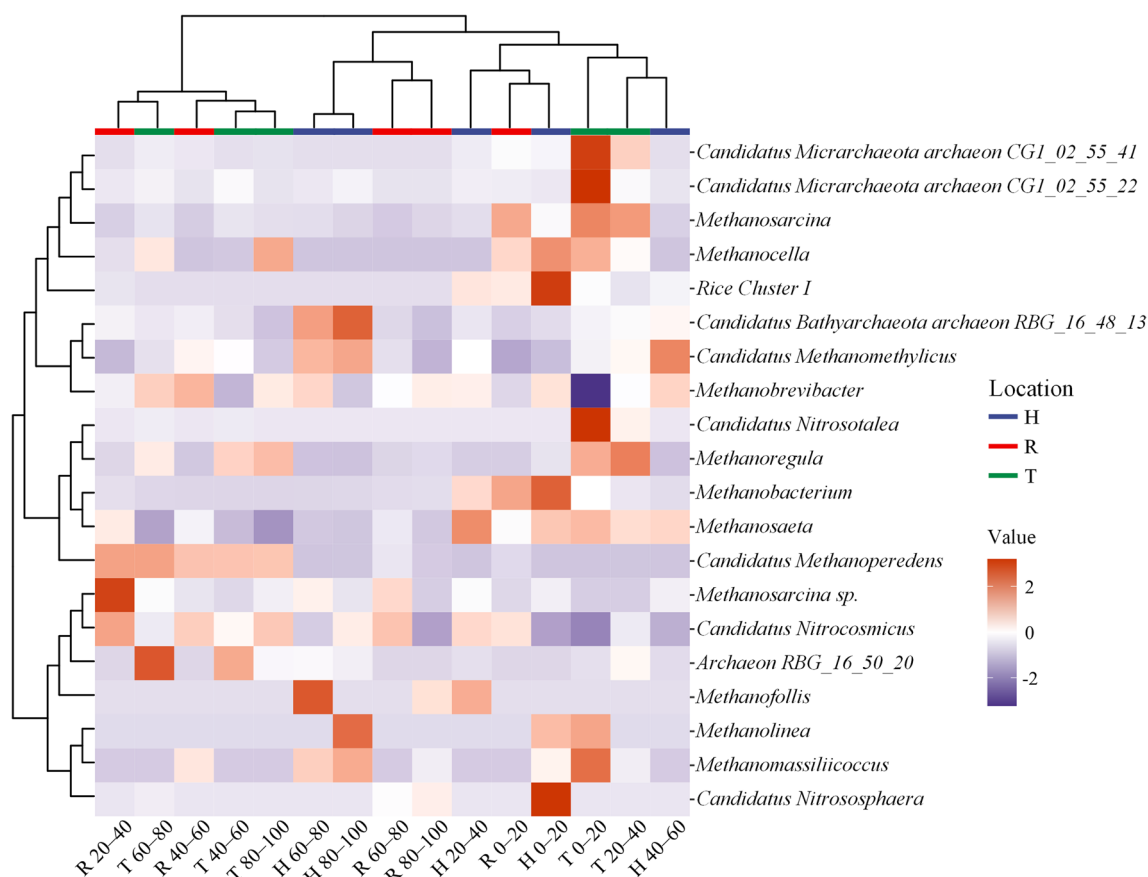


**Fig. 4** Heatmap of the abundances of the top 20 genera of archaea in the three peatlands. All data were normalized to obtain differentiation values. Different colors show the differences in the archaeal abundances in different peat samples. Red and purple colors represent relatively high and low abundances of the archaeal community, respectively. Bars with different colors at the top of the heatmap indicate different locations of peat samples. Specific locations and peat layers (cm) are reported on the x-axis. R, T, and H denote Ruokeba, Taishanmiao, and Hani, respectively

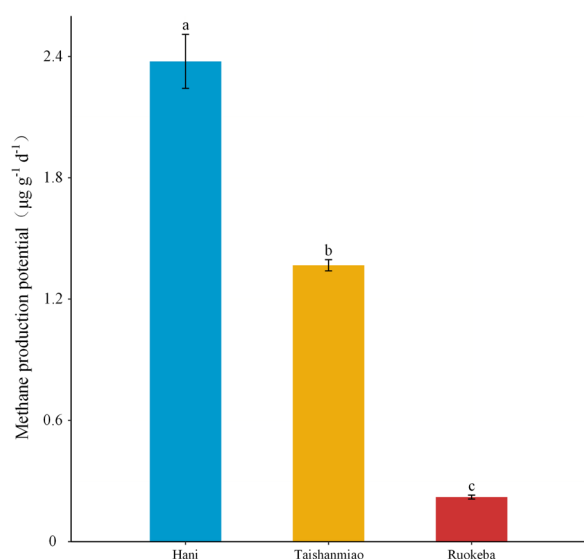


**Fig. 5** Methane production potentials in the three study peatlands. Different letters indicate significant differences in methane production potentials between peatlands ( $p < 0.05$ )

*Methanomassiliicoccales* was specific to the deep peat layer (60–100 cm) of R, showing qualitative correlations with C/N, pH, TC, WC, and TP, while *Methanobacteriales* and *Methanomicrobiales* were projected to the areas of H and R and were slightly correlated with WC, TFe, and C/N (Additional file 1: Fig. S1). *Nitrosotaleales* and *MBG-D/DHVEG-1* were observed in the T area and were correlated primarily with DOC, TP, TN, and TFe (Fig. S1), which is consistent with the archaeal distribution and correlation results (Figs. 3, 4, and 7). In addition, pH, TC, TN, and TFe were positively correlated with each other and negatively correlated with DOC and TP. Whereas TP was positively correlated with DOC and WC.

**Discussion**

**Comparison of the three peatlands**

The results obtained showed some similarities between the three peatlands. Indeed, all peatlands exhibited low pH values and high WC and TC (Table 1), corresponding

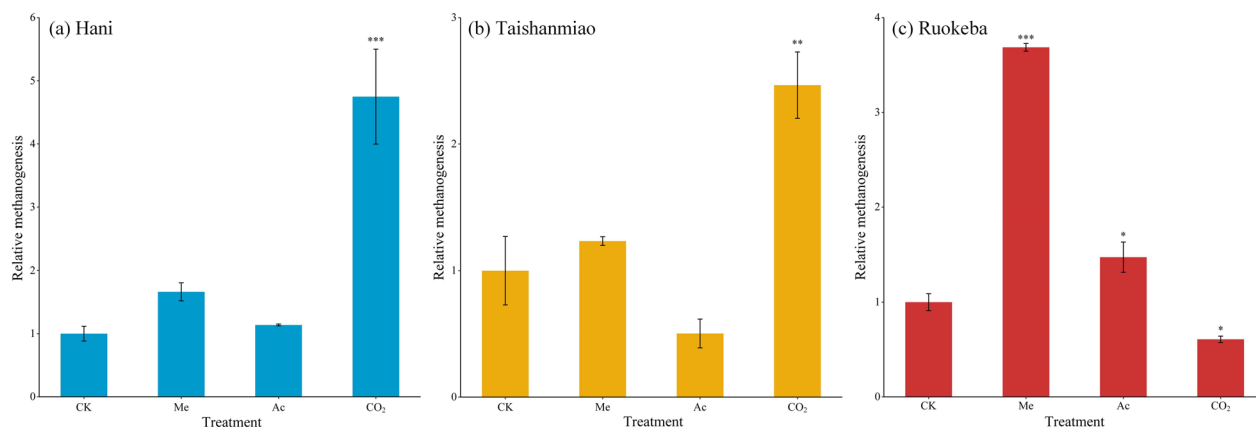


**Fig. 6** Relative methanogenesis in Hanj (a), Taishanmiao (b), and Ruokeba (c) peatlands under different substrate additions. \*, \*\*, and \*\*\* indicate significant differences in relative methanogenesis between treatments and control groups in each peatland at  $p < 0.05$ ,  $p < 0.01$ , and  $p < 0.001$ , respectively. Multiple comparisons were performed using Dunnett's method between control and treatment groups. CK, Me, Ac, and CO<sub>2</sub> represent control, methanol-addition, acetate-addition, and sodium bicarbonate/H<sub>2</sub>-addition groups, respectively

to the suitable environmental conditions for peatland development [13, 19]. In addition, the results showed similar C/N values, demonstrating the homogeneity of biochemical processes in the three peatlands. The peat physicochemical properties showed minor influences on dominant archaea (20.28%, Additional file 1: Fig. S1), suggesting other factors affecting the archaeal community in these peatlands, including climate, plant species, and hydrological characteristics [75–78].

The pH values and the TFe contents in R were higher than those observed in the remaining peatlands (Table 1). This finding might be due to the dominance of water recharge by groundwater, transporting numerous mineral substances, including Fe, that contribute to the pool of basic cations that could be consumed by eluviation [15, 24], thereby maintaining comparatively high pH values [22]. In addition, due to the input of mineral substances, silicon might release bound phosphorus, thereby increasing the available phosphorus contents [79, 80]. Therefore, besides groundwater-derived nutrient elements, TP contents were also higher in R than those in the other peatlands. The DOC contents in R were comparatively low (Table 1), which might be due to the pH and hydrological conditions. Low pH values favor the bonding of acidic elements to organic matter [81], while the hydrological characteristics can change

the DOC concentrations by affecting the input and output nutrients in peatlands [54]. Therefore, the minerotrophic fens could not accumulate DOC. Similarly, the increase in TC, TN, and C/N values with increasing peat depth suggested relatively strong microbial activity in deep peat layers in R (Table 1).

T is a *Sphagnum*-dominated ombrotrophic bog, exhibiting the lowest pH and TFe values and the highest DOC concentration (Table 1). The thickness of the peat layer in T can barely reach 1 m [27]. The results showed relatively low TC and TN contents in T (Table 1), which reflect its short development period. In addition, several peat physicochemical parameters showed significantly lower WC, DOC, C/N, TC, TN, and TP concentrations in the deeper peat layers than those observed in the surface peat layers (Table 1), suggesting the transition from peat to mineral soil and the weak biochemical activity in deeper peat layers. In addition, the unique karst landform in this area may also enhance groundwater recharge [26, 27], thereby promoting the release of mineral-bound phosphorus and, consequently, increasing phosphorus concentrations [79].

H is a typical poor fen characterized by negligible groundwater recharge [26]. Precipitation and surface runoff are the main water sources in H. In addition, the low infiltration rates often result in high groundwater levels above the peat surface [26, 51], explaining the highest WC in the three peatlands, as well as the high DOC and low TP contents (Table 1). H exhibited slight variations in the peat physicochemical parameters compared to the remaining peatlands (Table 1), suggesting stable biochemical processes and environmental changes in H.

**Table 2** Correlation coefficients between methane production potential (MPP), environmental factors, and relative abundances of methanogens

	WC	pH	DOC	<i>Methanomassiliicoccales</i>
MPP	0.759*	−0.811**	0.690*	−0.716*

\* and \*\* indicate significant correlations at  $p < 0.05$  and  $p < 0.01$ , respectively

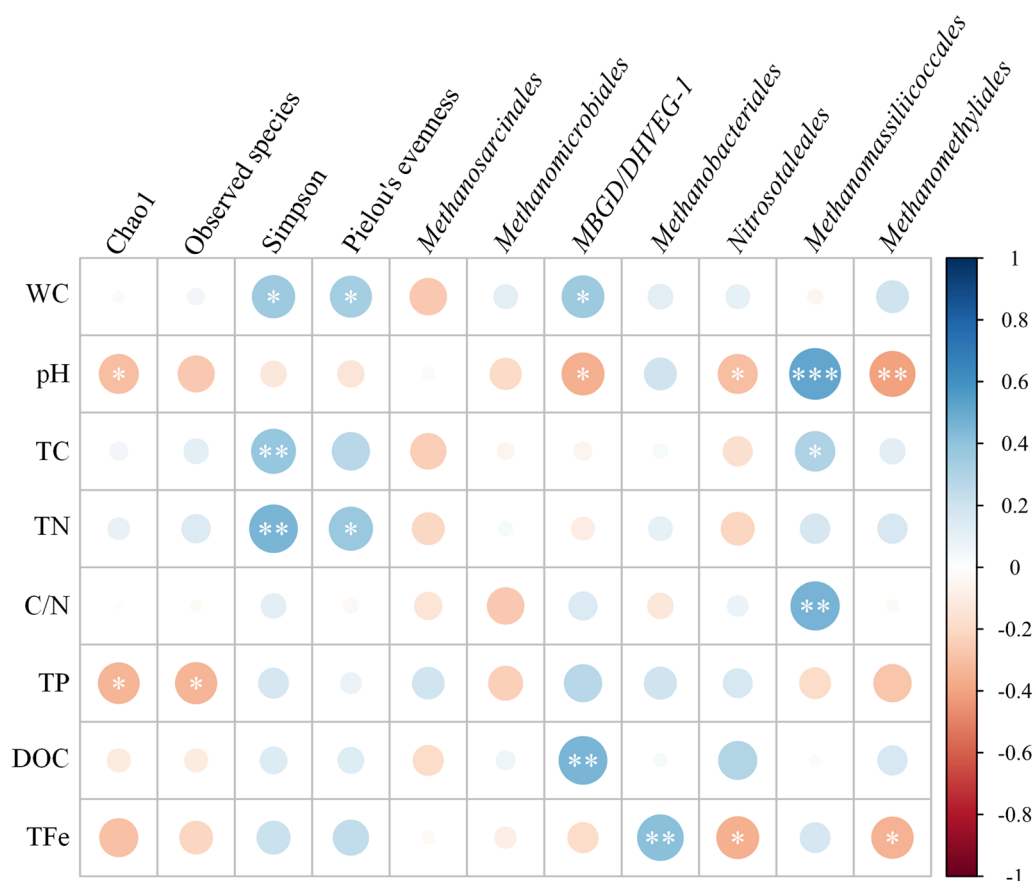


**Fig. 7** Correlations between physicochemical properties, archaeal community diversity indices, and abundances of dominant archaea. The depth of the color indicates the strength of each correlation. Red and blue colors indicate negative and positive correlation coefficients, respectively. The circle sizes reflect the significance of correlation coefficients. \*, \*\*, \*\*\* indicate significant correlation coefficients at  $p < 0.05$ ,  $p < 0.01$ , and  $p < 0.001$ , respectively. WC, TC, TN, TP, DOC, and TFe denote peat water content, total carbon content, total nitrogen content, total phosphorus content, dissolved organic carbon, and total Fe content, respectively

### Archaeal community characteristics and dominant species with corresponding methanogenesis pathways

NMDS ordination revealed the gradient-related differences in the archaeal community in the three peatlands, showing slight and substantial changes in the archaeal community in the surface and deep peat layers among three peatlands, respectively (Fig. 2), which is relatively consistent with the RDA analysis of dominant archaea (Additional file 1: Fig. S1) and the results reported in previous studies [82–84]. The ability of NMDS to reflect the differences in the archaeal community in different peatlands was further confirmed by the stress (0.116) and fitness results ( $R^2=0.986$  for nonmetric fit,  $R^2=0.929$  for linear fit, Fig. 2) of the model, supporting the area-depth differentiation of the archaeal community in the three peatlands. Minor et al. (2019) also indicated differences in the plant communities and nutrient concentrations between different peatland types [42]. The results of the present study showed great variations in the archaeal

community in T, which might be due to the large variation in the physicochemical properties in this peatland area (Table 1 and Fig. 2). The great impacts of peat physicochemical properties on the archaeal community structure ( $\alpha$ -diversity) were further investigated in this study. According to the obtained results, TC, TN, TP, WC, and pH were the main factors affecting the archaeal community structure (Fig. 7), corresponding to the fact that peatland is an N/P-limited ecosystem [15, 24]. According to the results of the present study, peatland types can be accurately distinguished based on their physicochemical properties, plant communities, and microbial communities.

According to the relative abundance results of dominant orders in the archaeal community, *Methanosarcinales* and *Methanomicrobiales* were the main methanogenic orders in peatlands, showing similar distribution patterns (Figs. 3 and 4) and average relative abundances of 8%, which is consistent with the results reported in previous

studies on peatlands in Yunnan Province, China, and Los Angeles, USA [83, 85]. The wide metabolic pathways and temperature growth ranges of these orders might be the main causes of their low correlations with environmental factors (Fig. 7) [33, 86, 87], suggesting their strong adaptability to the external environment. *Methanocellales* and *Methanofastidiosales* showed limited distributions in the three studied peatlands (Fig. 3). This finding might be because *Methanocellales* can only use  $H_2/CO_2$  or formate to produce  $CH_4$  in a temperature range of 15–40 °C [87], while *Methanofastidiosales* are strictly methylotrophic methanogen rarely distributed in nature [33, 88]. *Methanobacteriales*, which mainly use  $H_2/CO_2$  or some simple methyl compounds to produce methane [86, 87], were more abundant in the upper peat layers in H and R (Figs. 3, 4, and Additional file 1: Fig. S1). However, *Methanobacteriales* may exhibit a syntrophic relationship with certain bacteria, thereby coupling acetate oxidation and  $CH_4$  production processes [89]. Previous studies showed decreases in the abundance of bacteria with increasing peat depths as a result of decreases in the oxygen content [90, 91], and the syntrophic relationships between *Geobacter* and certain methanogens [92, 93], potentially explaining the high abundance of *Methanobacteriales* in the upper peat layers and the positive correlation between *Methanobacteriales* and TFe (Fig. 7). *Methanomassiliicoccales* and *Methanomethyliales* have similar metabolism pathways consuming methyl compounds [94, 95]. *Methanomassiliicoccales* were abundant in the 40–100 cm layer in R (Fig. 3 and Additional file 1: Fig. S1) and exhibited a strong positive correlation with pH (Fig. 7), suggesting that *Methanomassiliicoccales* are sensitive to acidic environments. Therefore, H and T might exhibit unsuitable conditions for *Methanomassiliicoccales* (Table 1). In contrast, *Methanomethyliales* were negatively correlated with pH (Fig. 7), suggesting good adaptation of this order to acidic environments. Indeed, the obtained results revealed a higher relative abundance of *Methanomethyliales* in H compared to those in the remaining peatlands (Figs. 3 and 4).

The heatmap of the archaeal distribution revealed that *Methanobacteriales*, *Methanomicrobiales* (*Methanofollis* and *Methanolinea*), *Methanocellales* (*Rice Cluster I* and *Methanocella*), and *Methanomethyliales* (*Candidatus Methanomethylicus*) were more abundant in H compared to other peatlands (Figs. 3 and 4), suggesting that hydrogenotrophic and methylotrophic were the major methanogenesis pathways in H [86, 87, 94, 95]. Whereas in R, *Methanomicrobiales*, *Methanomassiliicoccales* (*Methanomassiliicoccus*), and *Methanosarcinales* (*Methanosarcina* and *Candidatus Methanoperedens*) were the dominant methanogens (Figs. 3, 4, and Additional file 1: Fig. S1), indicating that methyl compounds and acetate were the

main substrates involved in the  $CH_4$  production process [87, 94]. The methanogenesis pathways in H and R were further investigated in this study by incubation experiments (Fig. 6a and c), indicating consistent results with the methanogenic composition (Figs. 3 and 4). Besides methanogens, *MBG-D/DHVEG-1* and *Nitrosotaleales* were also the dominant archaea in T (Figs. 3 and 6c). The relative abundance of these two archaea was about 78% of the methanogens in the 0–80 cm peat layer, which is considerably higher than that in the 80–100 cm peat layer in T (Fig. 3). The clustering results revealed a similar distribution of *Candidatus Bathyarchaeota RBG\_16\_48\_13* to those of *Candidatus Methanomethylicus*, *Methanobrevibacter*, and *Rice Cluster I* (Fig. 4), suggesting their similarity in terms of their ecological functions and environmental adaptation. Some recent studies have highlighted similar methanogenesis pathways of *Bathyarchaeota* species to those of some methanogens (e.g., *Methanomassiliicoccales*) [33, 86, 96]. In addition, these species are capable of performing anaerobic mineralization of proteins and anaerobic  $CH_4$  oxidation [97, 98]. The RDA and correlation analysis revealed negative relationships between pH and *MBG-D/DHVEG-1* and positive relationships between DOC and *MBG-D/DHVEG-1* (Fig. 7 and Additional file 1: Fig. S1), suggesting that *MBG-D/DHVEG-1* may be adapted to acidic environments of bogs and sensitive to activated carbon components. *Nitrosotaleales* are adapted ammonia-oxidizing archaea to acidic environments [99, 100], which are involved in the nitrogen cycle and nitrous oxide emissions in peatlands [101, 102]. Abundant *Nitrosotaleales* were also found in the Dajiuhu peatland near the study site in T [102], indicating the wide distribution of this archaea in this area, possibly due to the particular karst landform [26, 27]. The results of the present study highlighted the presence of some other unique archaea in T, including *Aenigmarchaeales*, *Thermoplasmatales*, and *Deep-Sea Euryarchaeotic Group (DSEG)* (Figs. 3 and 4), suggesting the special local situation. Therefore,  $CH_4$  production in T might not be only controlled by traditional methanogens but also by other unique archaea through hydrogenotrophic methanogenesis, as revealed by the incubation experiment (Fig. 6b).

#### Methanogenesis and its relationship with environmental factors and methanogens

The  $CH_4$  production potentials were significantly different between the three peatlands. The highest and lowest  $CH_4$  production potentials were observed in H and R, respectively (Fig. 5), which is consistent with the results reported in previous studies [43, 103, 104]. However, some studies conducted in boreal peatlands have indicated higher  $CH_4$  production in fens than in bogs [10, 43,

105]. In addition, other studies have revealed highly variable CH<sub>4</sub> production potentials in peatlands due to their strong heterogeneity [43, 44, 106–108]. Ye et al. [109] found the highest CH<sub>4</sub> production potential in the intermediate fen, which is similar to H. In contrast, Liu et al. [103] revealed extremely low and high CH<sub>4</sub> production potentials in Zoige peatland (near R) and Sanjiang Plain in China, respectively, using incubation experiments, showing increasing trends in the CH<sub>4</sub> production potential with increasing latitude. A previous study has also revealed high CH<sub>4</sub> production potentials in bogs than those in other peatland types [110]. Therefore, the peatland types do not naturally determine the CH<sub>4</sub> production potential.

The methanogenesis pathways in the different peatlands in our study, revealed by the archaeal community and incubation experiment results, are in line with the common rule (Figs. 3, 4, and 6) [23, 34, 111]. Generally, acetotrophic methanogenesis is dominant in minerotrophic fens, while methylotrophic methanogenesis occurs often in environments with high salt contents, such as marine and saline soda lakes where abundant methyl compound are available for methanogens [34, 62, 112, 113]. Previous studies have demonstrated that methanol is not the main substrate for CH<sub>4</sub> production in peatlands [89, 114, 115]. In contrast, other studies have demonstrated that methanol could be the main substrate for methanogenesis in cold environments [63, 116], even in *Sphagnum*-dominated bogs [117], which is consistent with the results shown in the present study (Fig. 6a and c), suggesting the occurrence of methylotrophic methanogenesis in cold peatlands with high latitude. In addition, the CH<sub>4</sub> production processes in H could be similar to that observed in T than R, even though there were some similar characteristics between H and R, such as methylotrophic methanogenesis. Some studies have shown that acetate can be formed from methanol through the fermentation process, thereby indirectly accelerating acetotrophic methanogenesis [62, 116]. However, our results were relatively inconsistent with these findings since the acetate addition in this study results in a minor enhancement effect on methane production, while the methanol addition significantly promoted methanogenesis in R (Fig. 6c).

The correlation analysis results highlighted a strong negative relationship between the pH values and CH<sub>4</sub> production potential (Table 2). Whereas the covariance analysis revealed a significant interaction effect between pH and study area on CH<sub>4</sub> production potential (Additional file 1: Tables S2 and S3), suggesting a variation in the pH effects among the three peatlands and is, therefore, a crucial and regional-specific factor controlling

CH<sub>4</sub> production potentials. This finding is, indeed, consistent with the results of previous studies investigating the pH impacts on the CH<sub>4</sub> production process, showing a great effect of pH on CH<sub>4</sub> production and the optimal pH for CH<sub>4</sub> production higher than that in situ [58, 109, 110, 118].

DOC represents the activated carbon component, which is easily utilized by microbes, thus influencing their activity [119, 120]. In this study, DOC concentration was positively correlated with the CH<sub>4</sub> production potential (Table 2). There are two mechanisms explaining the enhancement effect of DOC on CH<sub>4</sub> production. First, some DOC-derived compounds can directly accelerate CH<sub>4</sub> production [43, 121]; secondly, DOC inputs promote the reduction of Fe(III) [122], as well as the reduction of other electron acceptors, thereby mitigating the suppression effect caused by oxidized electron acceptors.

The results of the present study showed also a positive correlation between WC and CH<sub>4</sub> production potentials (Table 2). The WC can indirectly reflect the hydrological conditions, aeration, and oxygen contents in peatlands that affect the microbial community [41, 123–125]. The high WC in H was due to the high groundwater level [26]. Besides the high DOC concentrations, it can be concluded that H provides good environmental conditions for CH<sub>4</sub> production. However, oxidized materials can be transported to minerotrophic fens (e.g., R) through groundwater recharge, maintaining a comparatively stable redox potential in peatlands [126] and, consequently, inhibiting CH<sub>4</sub> production. The low DOC and WC values could be the main reasons explaining the lower CH<sub>4</sub> production potential in T than that in H (Table 1 and Fig. 5).

The influences of environmental factors on CH<sub>4</sub> production are attributed mainly to methanogens. In this study, although *Methanomassiliococcales* were the main methanogen that exhibited a negative correlation with CH<sub>4</sub> production potentials ( $R = -0.716$ , Table 2), this finding is considered unreliable due to the extremely low relative abundance of *Methanomassiliococcales* (<1%, Fig. 3). Whereas other methanogens and the total relative abundance of methanogens were not associated with CH<sub>4</sub> production potentials, showing the lack of correlation between the relative abundance of methanogens and CH<sub>4</sub> production potentials, which is consistent with the results reported in previous studies [46, 104, 127, 128]. For this weak correlation, it can be comprehended as that the presence of methanogens were not active enough to produce expected amount of methane, corresponding with the evidence of *mcrA* gene/transcript which better demonstrates the methanogenesis activity of methanogens [23].

Besides the possible lack of substrates for CH<sub>4</sub> metabolism in R, reflected by the low DOC contents (Table 1), the competition between different microbes could also be an important factor influencing methanogenesis. Vegetation in R consists mainly of grasses and sedges, which have substantially higher productivities than that of *Sphagnum* in the remaining peatlands [53, 129]. In addition, grasses and sedges can release photosynthetic carbon and increase oxygen concentrations in the rhizosphere [28, 83, 130, 131], thereby enhancing the activities of non-methanogen species [132] and, consequently, mitigating the activities of non-competitive methanogens [131, 133–135].

## Conclusions

This study demonstrated the similarities and differences in the archaeal community associated with CH<sub>4</sub> production in three typical peatlands in China, namely H, T, and R. The  $\beta$ -diversity of the archaeal community determined using NMDS revealed the differences in the archaeal community between the three peatlands, particularly in the deep peat layers. The mean relative abundance of methanogens in peat layers ranged from 10 to 12%, regardless of peatlands. In addition, the results showed high abundances of *Methanosarcinales* and *Methanomicrobiales* in all peat samples, while *Methanobacteriales* were distributed mainly in the upper peat layer (0–40 cm). Besides methanogens, *MBG-D/DHVEG-I*, *Nitrosotaleales*, and some other orders of *Bathyarchaeota* exhibited high abundances, particularly in T, which is characterized by unique geological conditions, highlighting the diversity of archaea in peatlands. The distribution of methanogens was generally in line with the respective methanogenesis pathways of the three peatlands. On the other hand, pH, DOC, and WC of peatlands were the main factors controlling CH<sub>4</sub> production potentials. However, no correlations were observed between methanogens and methane production potentials, suggesting the slight effect of relative abundances of methanogens on CH<sub>4</sub> production in peatlands. The combined effect of these physicochemical factors resulted in the highest and lowest CH<sub>4</sub> production potentials in H and R, respectively. In addition, the obtained results suggested that the peat physicochemical properties and archaeal community are important factors controlling methanogenesis in peatlands. Focusing on the ecological and biological aspects, this study provides a reference for investigating the relationship between the archaeal community and CH<sub>4</sub> production process in different types of peatlands in China, highlighting the importance of the archaeal community and peat physicochemical properties for studies on methanogenesis in peatlands.

## Supplementary Information

The online version contains supplementary material available at <https://doi.org/10.1186/s40793-023-00503-y>.

**Additional file 1: Table S1.** Detailed information of the three study peatlands. **Table S2.** Significances of interactions between study area and each index. **Table S3.** An example of analysis of covariance used in Table S2. **Fig. S1.** Redundancy analysis of peat physicochemical properties with dominant archaea.

## Acknowledgements

We acknowledge support from the Second Tibetan Plateau Scientific Expedition (2019QZKK0304), the Youth Innovation Promotion Association of the Chinese Academy of Sciences (2022376), the National Natural Science Foundation of China (42001093), the Youth Science and Technology Innovation Team Program of Sichuan Province of China (2021JDTD011), and the Youth Innovation Program of CIB (QNTS202201).

## Author contributions

Conceptualization: XC, DX, HC; Data curation: XC, DX; Formal analysis: XC, DX, HC; Funding acquisition: DX, HC; Investigation: XC, YW, QQ, LW, MW, JL, DX, HC; Methodology: XC, DX; Project administration: DX, HC; Supervision: DX, HC; Writing – original draft: XC, DX; Writing – review & editing: XC, DX, JL. All authors read and approved the final manuscript.

## Funding

This work was supported by the Second Tibetan Plateau Scientific Expedition (2019QZKK0304), the Youth Innovation Promotion Association of the Chinese Academy of Sciences (2022376), the National Natural Science Foundation of China (42001093), the Youth Science and Technology Innovation Team Program of Sichuan Province of China (2021JDTD011), and the Youth Innovation Program of CIB (QNTS202201).

## Availability of data and materials

Raw sequence data have been deposited in the Genome Sequence Archive (Genomics, Proteomics & Bioinformatics 2021) in the National Genomics Data Center (Nucleic Acids Res. 2022), China National Center for Bioinformation/Beijing Institute of Genomics, Chinese Academy of Sciences (GSA: CRA007847), publicly accessible at <https://ngdc.cncb.ac.cn/gsa>. Other data in this paper are available when requested.

## Declarations

### Ethics approval and consent to participate

Not applicable.

### Consent for publication

Not applicable.

### Competing interests

The authors declare that they have no known competing financial interests or personal relationships that could have appeared to influence the work reported in this paper.

### Author details

<sup>1</sup>CAS Key Laboratory of Mountain Ecological Restoration and Bioresource Utilization and Ecological Restoration Biodiversity Conservation Key Laboratory of Sichuan Province, Chengdu Institute of Biology, Chinese Academy of Sciences, No. 9, Section 4, South Renmin Road, Chengdu 610041, China. <sup>2</sup>Zoige Peatland and Global Change Research Station, Chinese Academy of Sciences, Hongyuan 624400, China. <sup>3</sup>School of Forestry and Horticulture, Hubei Minzu University, Enshi 445000, Hubei, China. <sup>4</sup>State Environmental Protection Key Laboratory of Wetland Ecology and Vegetation Restoration, Institute for Peat and Mire Research, Northeast Normal University, Changchun 130024, China. <sup>5</sup>SQE Department, COFCO Coca-Cola Beverages (Sichuan) Company Limited, Chengdu 610500, China. <sup>6</sup>CAS Center for Excellence in Tibetan Plateau Earth Sciences, Chinese Academy of Sciences (CAS), Beijing 100101, China. <sup>7</sup>University of Chinese Academy of Sciences, Beijing 100049, China.

Received: 8 March 2023 Accepted: 15 May 2023

Published online: 06 June 2023

## References

- Thomas CD, Cameron A, Green RE, Bakkenes M, Beaumont LJ, Collingham YC, et al. Extinction risk from climate change. *Nature*. 2004;427:145–8.
- Bousquet P, Ciais P, Miller JB, Dlugokencky EJ, Hauglustaine DA, Prigent C, et al. Contribution of anthropogenic and natural sources to atmospheric methane variability. *Nature*. 2006;443:439–43.
- IPCC. Climate Change 2014: Synthesis Report. IPCC, Geneva, Switzerland; 2014.
- Gedney N, Cox PM, Huntingford C. Climate feedback from wetland methane emissions. *Geophys Res Lett*. 2004;31:L20503.
- Limpens J, Berendse F, Blodau C, Canadell JG, Freeman C, Holden J, et al. Peatlands and the carbon cycle: from local processes to global implications—a synthesis. *Biogeosciences*. 2008;5:1475–91.
- Chen H, Zhu QA, Peng CH, Wu N, Wang YF, Fang XQ, et al. The impacts of climate change and human activities on biogeochemical cycles on the Qinghai–Tibetan Plateau. *Glob Change Biol*. 2013;19:2940–55.
- IPCC. Global Warming of 1.5 °C. Cambridge and New York: Cambridge University Press; 2018.
- Saunois M, Bousquet P, Poulter B, Peregon A, Ciais P, Canadell JG, et al. The global methane budget 2000–2012. *Earth Syst Sci Data*. 2016;8:697–751.
- Su J, Hu C, Yan X, Jin Y, Chen Z, Guan Q, et al. Expression of barley SUSIBA2 transcription factor yields high-starch low-methane rice. *Nature*. 2015;523:602–6.
- Derwent RG. Global warming potential (GWP) for methane: Monte Carlo analysis of the uncertainties in global tropospheric model predictions. *Atmosphere*. 2020;11:486.
- Zhang H, Tuittila ES, Korrensalo A, Laine AM, Uljas S, Welti N, et al. Methane production and oxidation potentials along a fen-bog gradient from southern boreal to subarctic peatlands in Finland. *Glob Change Biol*. 2021;27:4449–64.
- Lan X, Thoning KW, Dlugokencky EJ. Trends in globally-averaged CH<sub>4</sub>, N<sub>2</sub>O, and SF<sub>6</sub> determined from NOAA Global Monitoring Laboratory measurements. 2022. Accessed 15 Dec 2022.
- Page SE, Baird AJ. Peatlands and global change: response and resilience. *Annu Rev Environ Resour*. 2016;41:35–57.
- Page SE, Rieley JO, Banks CJ. Global and regional importance of the tropical peatland carbon pool. *Glob Change Biol*. 2011;17:798–818.
- Kolka R, Bridgman SD, Ping C. Soils of peatlands: histosols and gelsols. In: Vepraskas MJ, Craft CL, editors. *Wetlands soils: genesis, hydrology, landscapes and classification*. Boca Raton: CRC Press/Lewis Publishing; 2016. p. 277–309.
- Kirschke S, Bousquet P, Ciais P, Saunois M, Canadell JG, Dlugokencky EJ. Three decades of global methane sources and sinks. *Nat Geosci*. 2013;6:813–23.
- Zhu Q, Peng CH, Chen H, Fang XQ, Liu JX, Jiang H, et al. Estimating global natural wetland methane emissions using process modelling: spatio-temporal patterns and contributions to atmospheric methane fluctuations. *Glob Ecol Biogeogr*. 2015;24:959–72.
- Dean JF, Middelburg JJ, Röckmann T, Aerts R, Blauw LG, Egger M, et al. Methane feedbacks to the global climate system in a warmer world. *Rev Geophys*. 2018;56:207–50.
- Chen H, Wu N, Wang YF, Yang G, Ju PJ, Zhu D, et al. A historical overview about basic issues and studies of mires. *Sci Sin Terrae*. 2021;51:15–26.
- Charman DJ. Peat and peatlands. In: Likens GE, editor. *Encyclopedia of Inland waters*. Oxford: Academic Press; 2009. p. 541–8.
- Juottonen H, Galand PE, Tuittila ES, Laine J, Fritze H, Yrjala K. Methanogen communities and bacteria along an ecohydrological gradient in a northern raised bog complex. *Environ Microbiol*. 2005;7:1547–57.
- Ulanowski TA, Branfireun BA. Small-scale variability in Peatland pore-water biogeochemistry, Hudson Bay Lowland Canada. *Sci Total Environ*. 2013;454:211–8.
- Zalman C, Keller JK, Tfaily M, Kolton M, Pfeifer-Meister L, Wilson RM, et al. Small differences in ombrotrophy control regional-scale variation in methane cycling among *Sphagnum*-dominated peatlands. *Biogeochemistry*. 2018;139:155–77.
- Vitt DH. Peatlands. In: Jørgensen SE, Fath BD, editors. *Encyclopedia of ecology*. Amsterdam: Elsevier B.V; 2013. p. 557–66.
- Wang M, Liu ZG, Ma XH, Wang GD. Division of organic carbon reserves of peatlands in China. *Wetland Sci*. 2012;10:156–63.
- Cheng SG, Xiao H, Huang T, Zhou Y, Hu ZX, Liu XB. Paleoclimatic significances of peat humification in Hani of northeast China and regional comparison. *J Earth Sci Environ*. 2014;36:92–102.
- Wang H, Wu L, Xue D, Liu XF, Hong L, Mou L, et al. Distribution and environmental characteristics of *Sphagnum* peat bogs in Taishanmiao in Enshi City, Hubei Province. *Wetland Sci*. 2020;18:266–74.
- Laanbroek HJ. Methane emission from natural wetlands: interplay between emergent macrophytes and soil microbial processes. A mini-review. *Ann Bot*. 2010;105:141–53.
- Segers R. Methane production and methane consumption: a review of processes underlying wetland methane fluxes. *Biogeochemistry*. 1998;41:23–51.
- Bridgman SD, Cadillo-Quiroz H, Keller JK, Zhuang QL. Methane emissions from wetlands: biogeochemical, microbial, and modeling perspectives from local to global scales. *Glob Change Biol*. 2013;19:1325–46.
- Thauer RK, Kaster AK, Seedorf H, Buckel W, Hedderich R. Methanogenic archaea: ecologically relevant differences in energy conservation. *Nat Rev Microbiol*. 2008;6:579–91.
- Tahon G, Geesink P, Ettema TJG. Expanding archaeal diversity and phylogeny: past, present, and future. *Annu Rev Microbiol*. 2021;75:359–81.
- Duan CH, Zhang CJ, Sun YH, Li M. Recent advances on the novel methanogens. *Acta Microbiol Sin*. 2019;59:981–95.
- Conrad R. Importance of hydrogenotrophic, acetoclastic and methylotrophic methanogenesis for methane production in terrestrial, aquatic and other anoxic environments: a mini review. *Pedosphere*. 2020;30:25–39.
- Mayumi D, Mochimaru H, Tamaki H, Yamamoto K, Yoshioka H, Suzuki Y, et al. Methane production from coal by a single methanogen. *Science*. 2016;354:222–5.
- Conrad R. Contribution of hydrogen to methane production and control of hydrogen concentrations in methanogenic soils and sediments. *FEMS Microbiol Ecol*. 1999;28:193–202.
- Zhou Z, Zhang CJ, Liu PF, Fu L, Laso-Perez R, Yang L, et al. Non-synthetic methanogenic hydrocarbon degradation by an archaeal species. *Nature*. 2022;601:257–62.
- Yvon-Durocher G, Allen AP, Bastviken D, Conrad R, Gudasz C, St-Pierre A, et al. Methane fluxes show consistent temperature dependence across microbial to ecosystem scales. *Nature*. 2014;507:488–91.
- Veretennikova EE, Dyukarev EA. Diurnal variations in methane emissions from West Siberia peatlands in summer. *Russ Meteorol Hydrol*. 2017;42:319–26.
- Howard D, Agnan Y, Helmig D, Yang Y, Obrist D. Environmental controls on ecosystem-scale cold-season methane and carbon dioxide fluxes in an Arctic tundra ecosystem. *Biogeosciences*. 2020;17:4025–42.
- Minor MA, Ermilov SG, Philippov DAC. Hydrology-driven environmental variability determines abiotic characteristics and *Oribatida* diversity patterns in a *Sphagnum* peatland system. *Exp Appl Acarol*. 2019;77:43–58.
- Evans CD, Peacock M, Baird AJ, Artz RRE, Burden A, Callaghan N, et al. Overriding water table control on managed peatland greenhouse gas emissions. *Nature*. 2021;593:548–52.
- Ye R, Keller JK, Jin Q, Bohannon BJM, Bridgman SD. Peatland types influence the inhibitory effects of a humic substance analog on methane production. *Geoderma*. 2016;265:131–40.
- Rush JE, Zalman CA, Woerndle G, Hanna EL, Bridgman SD, Keller JK. Warming promotes the use of organic matter as an electron acceptor in a peatland. *Geoderma*. 2021;401: 115303.
- Wang J, Liu C, Gong X, Liu Y, Chen C. Trimethylamine stimulated and dissolved organic matter inhibited methane production in sediment from the Poyang Lake China. *Environ Technol*. 2016;37:2545–54.
- Hopple AM, Wilson RM, Kolton M, Zalman CA, Chanton JP, Kostka J, et al. Massive peatland carbon banks vulnerable to rising temperatures. *Nat Commun*. 2020;11:2373.

47. Koebsch F, Winkel M, Liebner S, Liu B, Westphal J, Schmiedinger I, et al. Sulfate deprivation triggers high methane production in a disturbed and rewetted coastal peatland. *Biogeosciences*. 2019;16:1937–53.
48. Griffiths NA, Hanson PJ, Ricciuto DM, Iversen CM, Jensen AM, Malhotra A, et al. Temporal and spatial variation in peatland carbon cycling and implications for interpreting responses of an ecosystem-scale warming experiment. *Soil Sci Soc Am J*. 2017;81:1668–88.
49. Shi G, Yan H, Zhang W, Dodson J, Hejnis H. The impacts of volcanic eruptions and climate changes on the development of Hani peatland in northeastern China during the Holocene. *J Asian Earth Sci*. 2021;210:104691.
50. Qiao SY. A preliminary study on Hani peat-mire in the west part of the Changbai Mountain. *Sci Geogr Sin*. 1993;13:279–87.
51. Cai C, Hong B, Zhu YX, Hong YT, Wang Y, Peng HJ. Holocene peat carbon accumulation and influence factors from the Hani peatland, northeast China. *Earth Environ*. 2013;41:597–604.
52. Wu Y, Xiang W, Fu XF, Li QL, Su J, Gong W, et al. Effect of phenolic acids derived from peatland on surface behavior of iron and its significance. *Earth Sci*. 2016;41:683–91.
53. Huang BX, Bai XZ, Yang XJ. Pollen record and paleovegetation evolution in 13.6 ka B. P. peat profile in Hongyuan area of Sichuan Province. *Shandong Land Resour*. 2012;28:1–4.
54. Olefeldt D, Roulet NT. Effects of permafrost and hydrology on the composition and transport of dissolved organic carbon in a subarctic peatland complex. *J Geophys Res Biogeosci*. 2012;117:15.
55. Gabriel GVM, Oliveira LC, Barros DJ, Bento MS, Neu V, Toppa RH, et al. Methane emission suppression in flooded soil from Amazonia. *Chemosphere*. 2020;250:126263.
56. Lowther JR. Use of a single sulfuric-acid hydrogen-peroxide digest for the analysis of pinus-radiata needles. *Commun Soil Sci Plant Anal*. 1980;11:175–88.
57. Kellogg LE, Bridgman SD. Phosphorus retention and movement across an ombrotrophic-minerotrophic peatland gradient. *Biogeochemistry*. 2003;63:299–315.
58. Wassmann R, Neue HU, Bueno C, Lantin RS, Alberto MCR, Buendia LV, et al. Methane production capacities of different rice soils derived from inherent and exogenous substrates. *Plant Soil*. 1998;203:227–37.
59. Medvedeff CA, Bridgman SD, Pfeifer-Meister L, Keller JK. Can *Sphagnum* leachate chemistry explain differences in anaerobic decomposition in peatlands? *Soil Biol Biochem*. 2015;86:34–41.
60. Fan L, Dippold MA, Ge T, Wu J, Thiel V, Kuzyakov Y, et al. Anaerobic oxidation of methane in paddy soil: role of electron acceptors and fertilization in mitigating CH<sub>4</sub> fluxes. *Soil Biol Biochem*. 2020;141:107685.
61. Duddleston KN, Kinney MA, Kiene RP, Hines ME. Anaerobic microbial geochemistry in a northern bog: acetate as a dominant metabolic end product. *Global Biogeochem Cycles*. 2002;16:1063.
62. Zhang G, Jiang N, Liu X, Dong X. Methanogenesis from methanol at low temperatures by a novel psychrophilic methanogen, *Methanobus psychrophilus* sp. nov., prevalent in Zoige wetland of the Tibetan Plateau. *Appl Environ Microbiol*. 2008;74:6114–20.
63. Ren MF, Li LY, Chen L, Xing TT, Liu YQ, Dong XZ. Methanogen communities and predominant methanogenic pathways in three saline-alkaline lakes on the Tibetan Plateau. *Acta Microbiol Sin*. 2020;60:161–71.
64. Keller JK, Takagi KK. Solid-phase organic matter reduction regulates anaerobic decomposition in bog soil. *Ecosphere*. 2013;4:54.
65. Bolyen E, Rideout JR, Dillon MR, Bokulich N, Abnet CC, Al-Ghalith GA, et al. Reproducible, interactive, scalable and extensible microbiome data science using QIIME 2. *Nat Biotechnol*. 2019;37:852–7.
66. Martin M. Cutadapt removes adapter sequences from high-throughput sequencing reads. *EMBnet J*. 2011;17:10–2.
67. Katoh K, Misawa K, Kuma K, Miyata T. MAFFT: a novel method for rapid multiple sequence alignment based on fast Fourier transform. *Nucleic Acids Res*. 2002;30:3059–66.
68. Faith DP. Conservation evaluation and phylogenetic diversity. *Biol Cons*. 1992;61:1–10.
69. Lozupone CA, Hamady M, Kelley ST, Knight R. Quantitative and qualitative beta diversity measures lead to different insights into factors that structure microbial communities. *Appl Environ Microbiol*. 2007;73:1576–85.
70. McDonald D, Price MN, Goodrich J, Nawrocki EP, DeSantis TZ, Probst A, et al. An improved Greengenes taxonomy with explicit ranks for ecological and evolutionary analyses of bacteria and archaea. *ISME J*. 2012;6:610–8.
71. Bokulich NA, Kaehler BD, Rideout JR, Dillon M, Bolyen E, Knight R, et al. Optimizing taxonomic classification of marker-gene amplicon sequences with QIIME 2's q2-feature-classifier plugin. *Microbiome*. 2018;6:90.
72. Kahm M, Hasenbrink G, Lichtenberg-Frate H, Ludwig J, Kschischko M. Gfrofit: fitting biological growth curves with R. *J Stat Softw*. 2010;33:1–21.
73. Wei T, Simko V. R package 'corrplot': Visualization of a correlation matrix (Version 0.92). 2021. <https://github.com/taiyun/corrplot>. Accessed 15 Dec 2022.
74. R Core Team. R: A language and environment for statistical computing. R Foundation for Statistical Computing, Vienna, Austria. 2020. <https://www.R-project.org>. Accessed 15 Dec 2022.
75. Walker TN, Garnett MH, Ward SE, Oakley S, Bardgett RD, Ostle NJ. Vascular plants promote ancient peatland carbon loss with climate warming. *Glob Change Biol*. 2016;22:1880–9.
76. Feng X, Deventer MJ, Lonchar R, Ng GHC, Sebestyen SD, Roman DT, et al. Climate sensitivity of peatland methane emissions mediated by seasonal hydrologic dynamics. *Geophys Res Lett*. 2020;47:e2020GL088875.
77. Kitson E, Bell NGA. The response of microbial communities to peatland drainage and rewetting. A review. *Front Microbiol*. 2020;11:582812.
78. Seward J, Carson MA, Lamit LJ, Basiliko N, Yavitt JB, Lilleskov E, et al. Peatland microbial community composition is driven by a natural climate gradient. *Microb Ecol*. 2020;80:593–602.
79. Ali MA, Lee CH, Kim PJ. Effect of silicate fertilizer on reducing methane emission during rice cultivation. *Biol Fertil Soils*. 2007;44:597–604.
80. Hömberg A, Broder T, Knorr KH, Schaller J. Divergent effect of silicon on greenhouse gas production from reduced and oxidized peat organic matter. *Geoderma*. 2021;386:114916.
81. Locky DA, Bayley SE, Vitt DH. The vegetational ecology of black spruce swamps, fens, and bogs in southern boreal manitoba. *Can Wetlands*. 2005;25:564–82.
82. Kim SY, Freeman C, Fenner N, Kang H. Functional and structural responses of bacterial and methanogen communities to 3-year warming incubation in different depths of peat mire. *Appl Soil Ecol*. 2012;57:23–30.
83. He S, Malfatti SA, McFarland JW, Anderson FE, Pati A, Huntemann M, et al. Patterns in wetland microbial community composition and functional gene repertoire associated with methane emissions. *MBio*. 2015;6:e00066.
84. Asemaninejad A, Thorn RG, Branfireun BA, Lindo Z. Vertical stratification of peatland microbial communities follows a gradient of functional types across hummock-hollow microtopographies. *Écoscience*. 2019;26:249–58.
85. Li W, Luo M, Shi R, Feng D, Yang Z, Chen H, et al. Variations in bacterial and archaeal community structure and diversity along the soil profiles of a peatland in Southwest China. *Environ Sci Pollut Res*. 2022;29:2276–86.
86. Cheng L, Zheng ZZ, Wang C, Zhang H. Recent advances in methanogens. *Microbiology China*. 2016;43:1143–64.
87. Angelidakis I, Karakashev D, Batstone DJ, Plugge CM, Stams AJ. Biomethanation and its potential. *Methods Enzymol*. 2011;494:327–51.
88. Nobu MK, Narihiro T, Kuroda K, Mei R, Liu WT. Chasing the elusive Euryarchaeota class WSA2: genomes reveal a uniquely fastidious methyl-reducing methanogen. *ISME J*. 2016;10:2478–87.
89. Horn MA, Matthies C, Kusel K, Schramm A, Drake HL. Hydrogenotrophic methanogenesis by moderately acid-tolerant methanogens of a methane-emitting acidic peat. *Appl Environ Microbiol*. 2003;69:74–83.
90. Vad CF, Horváth Z, Kiss KT, Tóth B, Péntek AL, Ács É. Vertical distribution of zooplankton in a shallow peatland pond: the limiting role of dissolved oxygen. *Annales de Limnologie Int J Limnol*. 2013;49:275–85.
91. Jiang L, Song YY, Sun L, Ma XY, Wang XW, Song CC, et al. Distribution of carbon and nitrogen cycle microbes along permafrost peatland profile in Northeast China. *Environ Prog Sustain Energy*. 2021;40: e13707.
92. Rotaru AE, Shrestha PM, Liu F, Markovait B, Chen S, Nevin KP, et al. Direct interspecies electron transfer between *Geobacter metallireducens* and *Methanosarcina barkeri*. *Appl Environ Microbiol*. 2014;80:4599–605.

93. Tang J, Zhuang L, Ma J, Tang Z, Yu Z, Zhou S. Secondary mineralization of ferrihydrite affects microbial methanogenesis in *Geobacter-Methanosarcina* Cocultures. *Appl Environ Microbiol*. 2016;82:5869–77.
94. Borrel G, Parisot N, Harris HMB, Peyretailade E, Gaci N, Tottley W, et al. Comparative genomics highlights the unique biology of methanomassiliicoccales, a thermoplasmatales optimizing taxonomic classification of marker-gene related seventh order of methanogenic archaea that encodes pyrrolysine. *BMC Genom*. 2014;15:679.
95. Vanwongerghem I, Evans PN, Parks DH, Jensen PD, Woodcroft BJ, Hugenholtz P, et al. Methylophilic methanogenesis discovered in the archaeal phylum Verstraetearchaeota. *Nat Microbiol*. 2016;1:16170.
96. Szuroczki S, Szabo A, Korponai K, Felfoldi T, Somogyi B, Marialigeti K, et al. Prokaryotic community composition in a great shallow soda lake covered by large reed stands (Neusiedler See/Lake Fert) as revealed by cultivation- and DNA-based analyses. *FEMS Microbiol Ecol*. 2020;96:15.
97. Lloyd KG, Schreiber L, Petersen DG, Kjeldsen KU, Lever MA, Steen AD, et al. Predominant archaea in marine sediments degrade detrital proteins. *Nature*. 2013;496:215–8.
98. Pierangeli GMF, Domingues MR, de Jesus TA, Coelho LHG, Hanisch WS, Pompeo MLM, et al. Higher abundance of sediment methanogens and methanotrophs do not predict the atmospheric methane and carbon dioxide flows in eutrophic tropical freshwater reservoirs. *Front Microbiol*. 2021;12:15.
99. Song YX, Wang BZ, Qin H, Kuang L, Tang XF, Wang XX, et al. Molecular phylogeny suggests a key role of atpase genes on evolutionary adaptation of soil ammonia-oxidizing Archaea to acid stress. *Acta Pedologica Sinica*. 2021;1136–1147.
100. Zhang LM, Hu HW, Shen JP, He JZ. Ammonia-oxidizing archaea have more important role than ammonia-oxidizing bacteria in ammonia oxidation of strongly acidic soils. *ISME J*. 2012;6:1032–45.
101. Siljanen HMP, Alves RJE, Ronkainen JG, Lamprecht RE, Bhattarai HR, Bagnoud A, et al. Archaeal nitrification is a key driver of high nitrous oxide emissions from arctic peatlands. *Soil Biol Biochem*. 2019;137: 107539.
102. Xu Y, Wang HM, Xiang X, Wang RC, Tian W. Vertical variation of nitrogen fixers and ammonia oxidizers along a sediment profile in the Dajihu peatland, central China. *J Earth Sci*. 2019;30:397–406.
103. Liu DY, Ding WX, Jia ZJ, Cai ZC. Relation between methanogenic archaea and methane production potential in selected natural wetland ecosystems across China. *Biogeosciences*. 2011;8:329–38.
104. Kolton M, Marks A, Wilson RM, Chanton JP, Kostka JE. Impact of warming on greenhouse gas production and microbial diversity in anoxic peat from a *Sphagnum*-dominated bog (Grand Rapids, Minnesota, United States). *Front Microbiol*. 2019;10:870.
105. Yavitt JB, Kryczka AK, Huber ME, Pipes GT, Rodriguez AM. Inferring methane production by decomposing tree, shrub, and grass leaf litter in bog and rich fen peatlands. *Front Environ Sci*. 2019;7:182.
106. Bienida A, Daté V, Andersen R, Nwaishi F, Price J, Mahmood MS, et al. Methane emissions from fens in Alberta's boreal region: reference data for functional evaluation of restoration outcomes. *Wet Ecol Manag*. 2020;28:559–75.
107. Tan W, Jia Y, Huang C, Zhang H, Li D, Zhao X, et al. Increased suppression of methane production by humic substances in response to warming in anoxic environments. *J Environ Manag*. 2018;206:602–6.
108. Sun T, Guzman JLL, Seward JD, Enders A, Yavitt JB, Lehmann J, et al. Suppressing peatland methane production by electron snorkeling through pyrogenic carbon in controlled laboratory incubations. *Nat Commun*. 2021;12:4119.
109. Ye RZ, Jin QS, Bohannon B, Keller JK, McAllister SA, Bridgman SD. pH controls over anaerobic carbon mineralization, the efficiency of methane production, and methanogenic pathways in peatlands across an ombrotrophic-minerotrophic gradient. *Soil Biol Biochem*. 2012;54:36–47.
110. Dunfield P, Knowles R, Dumont R, Moore TR. Methane production and consumption in temperate and sub-arctic peat soils—response to temperature and pH. *Soil Biol Biochem*. 1993;25:321–6.
111. Zhang L, Liu X, Duddlestone K, Hines ME. The effects of pH, temperature, and humic-like substances on anaerobic carbon degradation and methanogenesis in ombrotrophic and minerotrophic Alaskan peatlands. *Aquat Geochem*. 2020;26:221–44.
112. Galand PE, Fritze H, Conrad R, Yrjala K. Pathways for methanogenesis and diversity of methanogenic archaea in three boreal peatland ecosystems. *Appl Environ Microbiol*. 2005;71:2195–8.
113. Galand PE, Yrjala K, Conrad R. Stable carbon isotope fractionation during methanogenesis in three boreal peatland ecosystems. *Biogeosciences*. 2010;7:3893–900.
114. Yavitt JB, Lang GE. Methane production in contrasting wetland sites—response to organic-chemical components of peat and to sulfate reduction. *Geomicrobiol J*. 1990;8:27–46.
115. Blake LI, Tveit A, Ovreas L, Head IM, Gray ND. Response of methanogens in arctic sediments to temperature and methanogenic substrate availability. *PLoS ONE*. 2015;10: e0129733.
116. Jiang N, Wang Y, Dong X. Methanol as the primary methanogenic and acetogenic precursor in the cold Zoige wetland at Tibetan plateau. *Microb Ecol*. 2010;60:206–13.
117. Zalman CA, Meade N, Chanton J, Kostka JE, Bridgman SD, Keller JK. Methylophilic methanogenesis in *Sphagnum*-dominated peatland soils. *Soil Biol Biochem*. 2018;118:156–60.
118. Wang ZP, Delaune RD, Masscheleyn PH, Patrick WH. Soil redox and pH effects on methane production in a flooded rice soil. *Soil Sci Soc Am J*. 1993;57:382–5.
119. Qualls RG, Richardson CJ. Factors controlling concentration, export, and decomposition of dissolved organic nutrients in the Everglades of Florida. *Biogeochemistry*. 2003;62:197–229.
120. Kogel-Knabner I, Amelung W, Cao ZH, Fiedler S, Frenzel P, Jahn R, et al. Biogeochemistry of paddy soils. *Geoderma*. 2010;157:1–14.
121. Kim SY, Veraart AJ, Meima-Franke M, Bodelier PLE. Combined effects of carbon, nitrogen and phosphorus on CH<sub>4</sub> production and denitrification in wetland sediments. *Geoderma*. 2015;259:354–61.
122. Ye R, Horwath WR. Influence of rice straw on priming of soil C for dissolved organic C and CH<sub>4</sub> production. *Plant Soil*. 2017;417:231–41.
123. Iiyama I, Osawa K, Nagai T. A seasonal behavior of surface soil moisture condition in a reclaimed tropical peatland. *Soil Sci Plant Nutr*. 2012;58:543–52.
124. Fan ZS, Neff JC, Waldrop MP, Ballantyne AP, Turetsky MR. Transport of oxygen in soil pore-water systems: implications for modeling emissions of carbon dioxide and methane from peatlands. *Biogeochemistry*. 2014;121:455–70.
125. Song YY, Song CC, Hou AX, Sun L, Wang XW, Ma XY, et al. Temperature, soil moisture, and microbial controls on CO<sub>2</sub> and CH<sub>4</sub> emissions from a permafrost peatland. *Environ Prog Sustain Energy*. 2021;40: e13693.
126. Thompson Y, Sandefur BC, Karathanasis AD, D'Angelo E. Redox potential and seasonal porewater biogeochemistry of three mountain wetlands in southeastern Kentucky, USA. *Aquat Geochem*. 2009;15:349–70.
127. Liebner S, Ganzert L, Kiss A, Yang S, Wagner D, Svenning MM. Shifts in methanogenic community composition and methane fluxes along the degradation of discontinuous permafrost. *Front Microbiol*. 2015;6:356.
128. Tong C, She CX, Yang P, Jin YF, Huang JF. Weak correlation between methane production and abundance of methanogens across three brackish marsh zones in the Min River Estuary China. *Estuar Coasts*. 2015;38:1872–84.
129. Zeng J, Chen H, Liu JL, Yang SZ, Yan F, Cao Q, et al. The decrease of peatland water table on the Qinghai–Tibet Plateau caused the increase of soil phenolic substances and vegetation biomass which promoted the accumulation of soil carbon. *Acta Ecol Sin*. 2022;42:625–34.
130. Rupp D, Kane ES, Dieleman C, Keller JK, Turetsky M. Plant functional group effects on peat carbon cycling in a boreal rich fen. *Biogeochemistry*. 2019;144:305–27.
131. Conrad R. Control of microbial methane production in wetland rice fields. *Nutr Cycl Agroecosyst*. 2002;64:59–69.
132. Sutton-Grier AE, Megonigal JP. Plant species traits regulate methane production in freshwater wetland soils. *Soil Biol Biochem*. 2011;43:413–20.
133. Agethen S, Sander M, Waldemer C, Knorr KH. Plant rhizosphere oxidation reduces methane production and emission in rewetted peatlands. *Soil Biol Biochem*. 2018;125:125–35.
134. Mandic-Mulec I, Ausec L, Danevcic T, Levicnik-Hofferle S, Jerman V, Kraiger B. Microbial community structure and function in peat soil. *Food Technol Biotechnol*. 2014;52:180–7.
135. Turner JC, Moorberg CJ, Wong A, Shea K, Waldrop MP, Turetsky MR, et al. Getting to the root of plant-mediated methane emissions

and oxidation in a thermokarst bog. *J Geophys Res Biogeosci.* 2020;125:e2020JG005825.

### **Publisher's Note**

Springer Nature remains neutral with regard to jurisdictional claims in published maps and institutional affiliations.

**Ready to submit your research? Choose BMC and benefit from:**

- fast, convenient online submission
- thorough peer review by experienced researchers in your field
- rapid publication on acceptance
- support for research data, including large and complex data types
- gold Open Access which fosters wider collaboration and increased citations
- maximum visibility for your research: over 100M website views per year

**At BMC, research is always in progress.**

Learn more [biomedcentral.com/submissions](https://biomedcentral.com/submissions)

